Journal of Materials Chemistry A

Accepted Manuscript

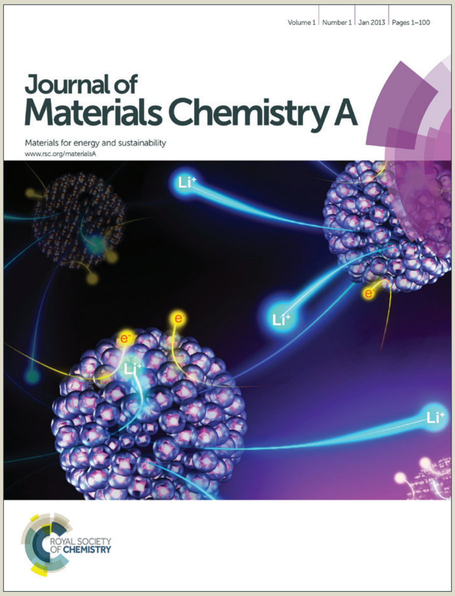

ROYAL SOCIETY OF CHEMISTRY

www.rsc.org/materialsA

Recent Advances in Metal Nitrides as High-Performance Electrode Materials for Energy Storage Devices

Muhammad-Sadeeq Balogun,[a] *Weitao Qiu,*[a] *Wang Wang,*[a] *Pingping Fang,*[a] *Xihong Lu,*[a]** and Yexiang Tong*[a]***

[a] *KLGHEI of Environment and Energy Chemistry, MOE of the Key Laboratory of Bioinorganic and Synthetic Chemistry, School of Chemistry and Chemical Engineering, Sun Yat-Sen University, Guangzhou 510275, People's Republic of China.*

E-mail: luxh6@mail.sysu.edu.cn; chedhx@mail.sysu.edu.cn

Abstract:

Energy storage devices are the key components for the successful and sustainable energy systems. Some of the best types of energy storage devices right now include lithium-ion batteries and supercapacitors. Research in this area has greatly improved electrode materials, enhanced electrolytes, and conceived clever designs for device assemblies with the ever-increasing energy and power density for electronics. Electrode materials is the fundamental key component for energy storage devices that largely determine the electrochemical performance of the energy storage devices. Various materials such as carbon materials, metal oxides and conducting polymers has been widely used as electrode materials for energy storage devices, and great achievements has been made. Recently, metal nitrides has attracted increasing interests as remarkable electrode material for lithium-ion batteries and supercapacitors due to their outstanding electrochemical property, high chemical stability, standard technological approach and extensive fundamental importance. This review analyzes the development and progress of metal nitrides as suitable electrode materials for lithium-ion batteries and supercapacitors. The challenges and prospects of metal nitrides as energy storage electrode materials is also discussed.

1. Introduction

The requirement for alternative and sustainable sources of power becomes more urgent as we move further into the 21st century. [1] Clean, inexpensive, and safe high energy and power density materials are required to enable the generation, storage, and conversion of (principally electrical) energy via non-polluting processes. Energy storage is accomplished by devices or physical media that store energy to perform useful operation. The energy present at the initial formation of the universe has been stored in stars such as the sun, and is now being used by humans directly (e.g. through solar heating), or indirectly (e.g. by growing crops or conversion into electricity in solar cells). In order to meet the desire for an efficient and clean power source fitting the development of peoples' daily life and production, scientists have never given up trying to improve the electrochemical performance of existing energy storage device techniques. [2]

Among the technologies for near-future energy storage are rechargeable lithium-ion batteries, fuel cells, and supercapacitors (SCs). [3] In the past two decades, lithium ion batteries (LIBs) have achieved great successes due to their superior comprehensive battery performance, compared to lead–acid, Ni–Cd and Ni–MH battery. However, like the previous battery techniques, its development has also met a bottleneck recently. [4] Supercapacitors (SCs) bridge the gap between conventional capacitors and rechargeable batteries. Within SCs, the electrolyte is the conductive connection between the two electrodes, distinguishing them from electrolytic capacitors, in which the electrolyte only forms the cathode. Fuel cells (FCs) are device that converts the chemical energy from a fuel into electricity through a chemical reaction with oxygen or another oxidizing agent.

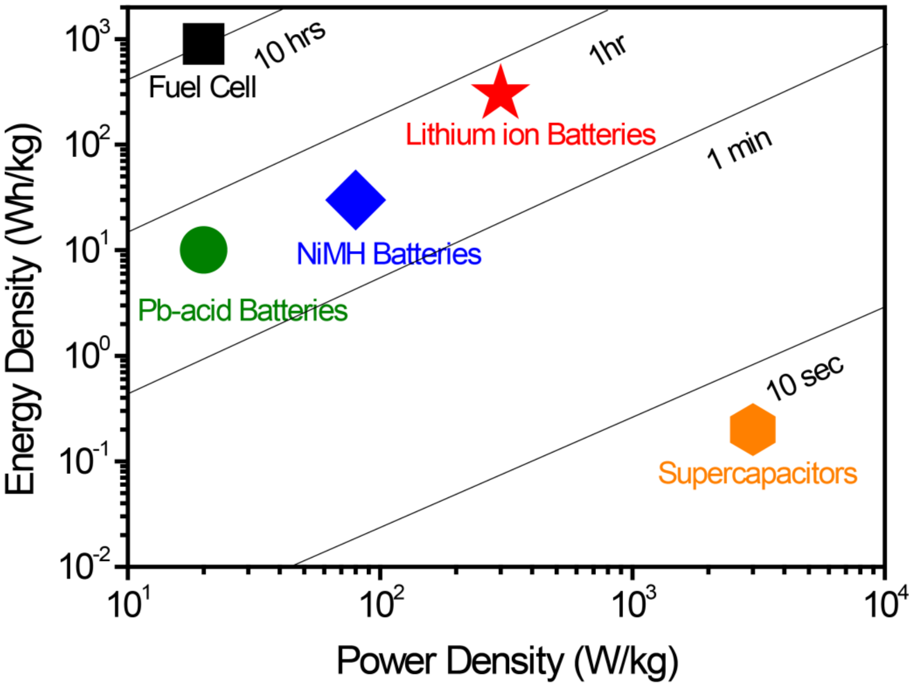

Figure 1. Ragone plot for commonly available energy storage devices [5]

To meet up with the requirement for the near-future energy storage device, high power and energy density energy storage devices call for consideration. Comparing the performance of different energy storage devices, Figure 1 illustrates the energy density of energy storage devices as a function of power density, known as "*Ragone plot*". [5] Fuel cells possesses high energy density but low power density, SCs were observed to have higher power density but low energy density and LIBs with average power and energy density when compare to Fuel cells and SCs. Thus, the development of high energy and power energy storage device is highly pursued.

With respect to improving the high consumption of energy by humans, electrode materials applied in these energy storage devices becomes vigorously important. They put forward higher requirements on the state-of-the-art rechargeable LIBs and SCs in the aspect of not only charge/discharge performance, but also safety, cost, sustainability and environmental friendliness. [6] In recent years, substantial efforts have been made to the explorations of novel electrode materials for LIBs and SCs with attractive specific capacity (capacitance) excellent cycling stability. [7, 8] There are several potential advantages and disadvantages associated with the development of electrodes for energy storage devices. Shortly, materials for LIBs include positive electrode named “Cathode” and negative electrode termed “Anode”. From the past and recently, carbon and carbon based materials, [9-13] metal oxides, [14-17] nitrides, [18, 19] carbides, [20-23] and their composites [24-27] have been employed as anode materials for LIBs. With respect to cathode materials, Almost all the research and commercialization has centered on the layered compounds with an anion close-packed or almost close-packed lattice like $LiCoO_2$, [28, 29] $LiMnO_2$, [30, 31] and the transition-metal phosphates, such as the olivine $LiFePO_4$. [32, 33] In SCs, carbonaceous materials, conducting polymers, metal oxides and composites of these aforementioned materials are the common electrode materials that have been employed extensively. For examples, carbonaceous materials such carbon nanotubes and graphene, [34-37] conducting polymers such as PANI, [38,Arbizzani, 2001 #42] polypyrrole, [39]metal oxides such as MoO_2, [40, 41] MnO_2, [42] carbon nanocomposites, [43-46] metal oxide composites, [47] and so on have all been reported as electrode materials for SCs.

The demand and type of electrode materials has been briefly discussed above and the progresses in the development of these electrode materials are well summarized. [7, 27, 48-53] Recently, in addition to carbon and metal oxides, metal nitrides have been also employed as high-performance electrode materials for LIBs and SCs due to their high specific capacities, high electrical conductivity, high chemical and thermal stability and have been used widely as electrodes in energy storage devices. As promising electrode materials, most metal nitrides such as TiN, VN. Mo_2N, MoN, FeN, Ni_3N, NbN, Ta_3N and so on, are often use as anode materials in LIB and SCs. Up till date, only $LiMoN_2$ have once be reported as LIB cathode. [54] Particularly, transition metal nitrides are also of great interest because of their capability of storing lithium by the conversion mechanism. Most of the developed metal nitrides such as TiN, [55] VN, [56] Mo_2N, [57] FeN, [58] Ni_3N, [59] NbN, [60] Ta_3N, [61]and so on, are often use as anode materials in LIB and SCs, while only $LiMoN_2$ have once been reported as LIB cathode. [54] In this review, we will summarize the progress of metal nitrides as electrode materials for LIBs and SCs. Also, the syntheses of some of these metal nitrides were also discussed. Furthermore, we will also discuss the current challenges of the metal nitrides as electrode materials in LIBs and SCs.

2. General Synthesis of Metal Nitrides

The significant and rapid progress in nitride chemistry has been seen over the last decade or so with improved classification and development of new synthetic routes leading to new nitride materials. The synthesis of nitrides is still very complex with large thermodynamic barriers which occur from the making and breaking of N≡N bonds (945 kJ/mol for N≡N compared to 498 kJ/mol for O=O). Many nitrides, especially those containing s-block elements, are air and moisture sensitive, and rapidly form oxides, hydroxides and ammonia upon contact with oxygen or moisture. These factors can therefore contribute to the low abundance of nitride compounds, compared to those of the oxides or carbides. For most of the twentieth century, the chemistry of binary and ternary nitrides progressed very slowly, in marked contrast to the chemistries of metal oxides or fluorides. In major part, this slow development can be traced to the limited synthesis routes available, the direct route from the elements is limited by the great strength of the triple bond in dinitrogen which means that only highly thermally stable nitrides can be made by this method. Other routes from nitrogen compounds including ammonia or azides were limited to specific classes of compound and resulting purities were sometimes poor. The known nitrides were often intractable, inert and difficult to characterize. [62]

Briefly, several methods have been developed in synthesizing metal nitrides. [63] (a) Heating metals or samples mixed with carbon to high temperatures in N_2 or NH_3 environments and examining the recovered products has resulted in much of our current knowledge of transition metal nitride compounds and their phase relations [64] and these techniques usually lead to formation of lower nitride materials. (b) High pressure and temperature synthesis approaches is also a way to synthesize metal nitrides. [65-67] (c) Ammonolysis of binary compounds, which involves the reactions of simple compounds such as chlorides, oxides and sulfides with ammonia often produce nitrides, with the advantage of of avoiding sinterable metals. [68] This method have been employed by Choi and Kumta in the synthesis of Ta_3N_5 and WN. [61] (d) Ammonolysis of oxides, which which involves heating the metal oxide directly in flowing NH_3 while slowly raising the temperature. Such preparation method have been employed by Lu's group in the synthesis of TiN and VN. [69-71] (e) Vapor deposition of films, in which many of the most important nitride materials are films deposited from the vapor phase by PVD, CVD and related techniques. [68] Transition metal nitrides are widely used in thin film form and typically are nano- or microcrystalline as deposited. [56, 69, 70] Other methods include solid state metathesis reactions (used in preparing alkali and alkaline-earth metal nitrides), [71-74] solvothermal synthesis (employed in the the fabrication of Al group), [75] sol-gel processing, [76-78] theoretical predictions developed by Kroll et al. [79-81] and so on.

3. Metal Nitrides for Lithium Storage

As metal nitrides are emerging as a new and promising electrode material for high-performance LIBs, [8, 82] due to their excellent electrical conductivity {Lu, 2012 #6} and their low and flat potentials close to that of lithium metal, [83] there is need for a comprehensive account of such development. Metal nitrides are promising electrode materials due to their high Li ion diffusion. The metal nitride system reveal ordered and disordered phases with significant levels of lithium vacancies, [84] because Li vacancies are the charge carriers in Li_3N, which is a well-known fast ion conductor with the highest Li^+ conductivity observed in a crystalline solid electrolyte at ambient temperature. [84] The formation of additional vacancies in the nitride phases implies a potential for enhanced lithium ion diffusion. The Li ion diffusivity in metal nitrides consist of inter and intralayer diffusion. The calculated Li ion diffusion of the parent compound (Li_3N) is 9.02×10^{-14} m^2/s [84] and some metal reported metal nitrides include 2.7×10^{-14} m^2/s for $Li_{3-x-y}Cu_xN$, [85] 5.40×10^{-10} m^2/s for $LiMn_3N_2$, [70] 0.638×10^{-14} m^2/s for LiNiN [84] and so on. Thus, metal nitrides also offer suitable kinetic reaction, due to the fast diffusion of Li ions as a result of the Li vacancies after conversion reaction, leading to relatively high power densities. [83, 85]

Generally, netal nitrides exist in two kinds namely lithium transition metal nitrides and single metal nitrides. [70, 86] These two kinds of metal nitrides have been widely studied and reported to be indexed to conversion reaction mechanism, undergoing intercalation and deintercalation with lithium and also exhibit good performance as electrode material in LIBs in the early studies. [54, 69]

3.1. Lithiated Metal Nitrides

Series of alternative anodes with the improved capacity density and enhanced thermal safety have been highly investigated as substitute for the commercial graphite in LIBs. Among them, Li-alloys and lithium transition metal nitrides appear to be the most promising candidates in terms of their reversible capacities and reactive potentials. [1] However, the structural instability caused by the volume effects seriously hinders the possible application of Li-alloys. The substitution of the transition metal has important consequences for the physical properties [85, 87] and it has been shown that substitution of an aliovalent transition metal increases the conductivity in the nitride. [88] These kinds of nitrides are called "*Lithiated Metal Nitrides*". The first lithiated metal nitride was $LiMoN_2$ by Elder and his Co-workers. [54] $LiMoN_2$ was demonstrated as a cathode material with voltage range of 2.7 – 4.2 V because of two pseudoplateaus located at an average voltage of 3.73 and 4.07 V. A capacity of about 110 mAh/g was delivered by the $LiMoN_2$ electrode. During the discharge processes of the $LiMoN_2$, Li_3N and Mo atom were formed. Lithiated metal nitrides were mostly considered as LIB electrode materials due to the formation of Li_3N when they come in contact with Li ions. [89-91] In LIBs, when metal nitrides come in contact with Li ion, two reaction processes will likely occur; (1) Li ion will be located in the metal nitride layer and (2) Li ion also located between the metal nitride layers. [89, 90] Li_3N, which dominated the nitride chemistry structure, has been a promising electrode material for LIBs based on the two reaction processes.

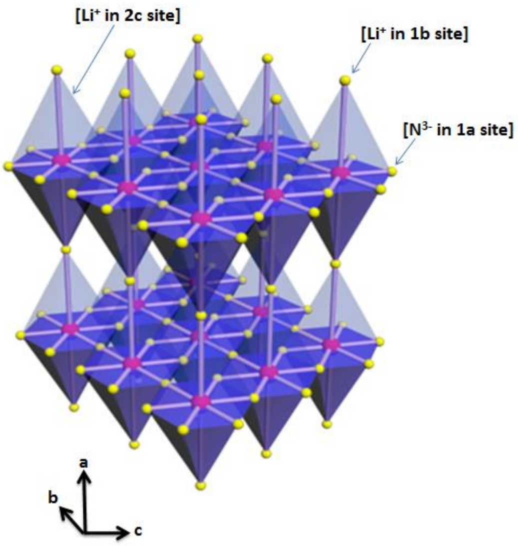

Figure 2. Structure of Lithium Nitride. Purple spheres (Li), Yellow Spheres (N), hexagonal bipryamidal structure space group P6/mmc. [92]

Figure 2 shows the typical crystal structure of cubic Li_3N. This structure shows that Li_3N consist of a nitrogen atom surrounded by eight Li atoms and six Li atoms in the same plane, trigonally coordinated to the nitrogen atom, and one linearly coordinated to the nitrogen atom above and below the plane. Thus, they form a hexagonal bipyramid [92] which shows an obvious effect upon the electrochemical behavior of the hexagonal nitrides in the Li extraction stage. [93] Newly developed lithium layer nitrides were anodes because their Li intercalation voltage plateau lies below 2 V. [94-98] For instance, Nishijima *et al*. and Cabana *et al*. prepared Li_7MnN_4 with a discharge capacity of 210 mAh/g and 180 mAh/g, respectively both displaying Li intercalation at about 1.1 V and Li de-intercalation at 1.3 V. [99, 100] Wen *et al*. achieved a discharge capacity of 400 mAh/g at 0.3 mA/cm^2 after 50 cycles for lithium silicon nitride showing Li insertion and extraction at 0.5 V and 1.2 V respectively. [101] Higher discharge capacity of over 500 mAh/g was reported by Rowsell *et al*. for layered $Li_{2.7}Fe_{0.3}N$ due to two Li insertion voltage plateaus at 0.4 V and 1.18 V, [86]

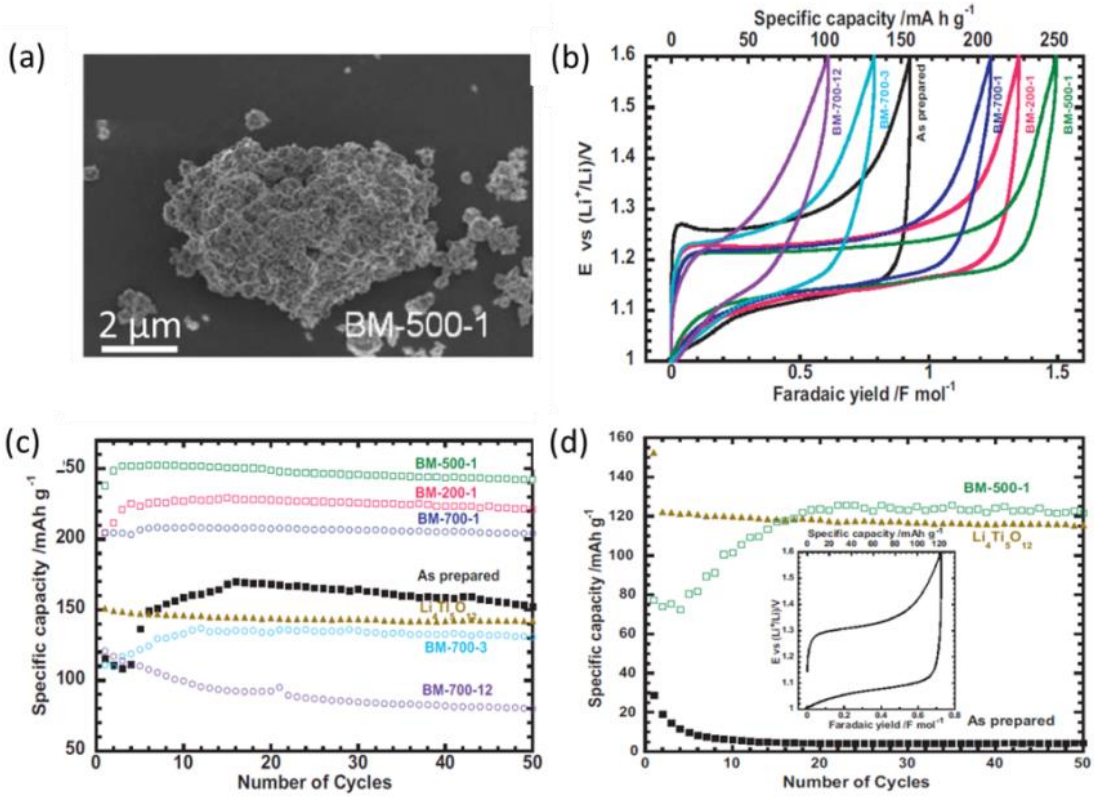

Figure 3. (a) SEM micrographs of ball-milled Li_7MnN_4. (b) charge–discharge curves for cycle 10 at C rate in the 1.6 V–1 V potential range. (c) Evolution of specific capacity as a function of the number of cycles. (d) Specific capacity vs. cycle number at 5 C rate for BM-500-1for the as prepared sample and for a $Li_4Ti_5O_{12}$ commercial sample. Inset: typical charge–discharge curves for BM-500-1 at 5 C for cycle 20. Reproduced from Ref. [102] with permission from Elsevier.

Recently, Bach and his co-workers studied the influence of structure and ball-milling on the electrochemical properties of Li_7MnN_4 at 1 C rate (Figure 3).[102] SEM image shows that the ball milled Li_7MnN_4 sample consist of small particle of a few µm from 2 to 5 µm (Figure 3a). Li intercalation was observed at a voltage plateau of 1.14 and 1.2 V (Figure 3b). Significantly, the ball-milled sample improved the specific capacity with about 60% increment (250 mAh/g) when compared with the as-prepared sample (150 mAh/g) (Figure 3c). Even at high current rate of 5 C, the ball-milled sample exhibited a stable capacity *vs.* cycles, around 120 mAh/g, which is well comparable to the behavior achieved for $Li_4Ti_5O_{12}$ (Figure 3d). However, despite many efforts to achieve lithiated nitrides with high stability, the capacity fading in them appears to be the major predicament which is related to the electrochemical instability under high Li extraction and the interfacial incomparability cause by the decomposition of the passive film on the surface of the active hosts. [103] In this way, studies of the electrochemical behavior of the quadruple lithiated metal nitrides have been reported. The morphology characteristic of quadruple lithiated metal nitrides has an obvious influence upon the electrochemical stability of the compounds in the Li-extraction stage and as lithium storage hosts. [93] Thus, low cost lithium transition metal nitrides with the improved cyclability can be developed. For example, the expensive Co can be replaced partially by Ni and Cu. Liu *et al*. demonstrates the electrochemical performance of $Li_{2:6}Co_{0:2}Cu_{0:2}N$, $L_{i2:5}Co_{0:2}Cu_{0:1}Ni_{0:1}N$ and $Li_{2:6}Co_{0:2}Cu_{0:15}Fe_{0:05}N$ as LIBs anode. [93] This research reveals that these compounds show large reversible capacities of about 700–900 mAh/g at 0.15 mA/cm^2 and excellent capacity retention due to electrochemical stability associated to the Li-extraction degree and the enhanced interfacial compatibility as a result of Ni substitution. The resulting electrochemical performance was also better than the pristine lithiated cobalt nitride with reversible capacity retention of 400 mAh/g. [93] From the economical perspective, lithium is not readily available and quite limited in the earth crust. [104] It was believed that the lithium already available in the electrolyte

($LiPF_6$, $LiClO_4$) is enough for lithium intercalation and hence, ternary nitrides without lithiation such as $Cr_{1-x}Fe_xN$, was reported by Qian and Zheng for the first time. [58] A reversible capacity above 1000 mAh/g was accounted for $Cr_{1-x}Fe_xN$ which is much higher than the lithiated nitrides. Their potential application was limited due to the large polarization of Cr.

3.2. Single Metal Nitrides for Lithium Storage

The development of single metal nitride thin films (also known as binary metal nitrides) as LIB electrode materials becomes rampant in the 2000's due to their average reversible capacity and stability [105] and were also reported to possess better electrochemical properties than the corresponding lithiated metal nitrides. [106] The binary metal nitrides have the ability to reduce the huge volume expansion, and hence a better cycling performance. [70] Lithiated metal nitrides involve calcining mixture of Li_3N and the transition metal powders while single nitrides requires a direct deposition of the metal nitride powders on a thin film substrate. Primarily, single metal nitrides materials are based on the binary compound formed readily between a metal and nitrogen such as lithium and nitrogen. As mentioned above, alkali metal nitrides are dominated by Li_3N which is known to have high lithium-ion conductivity (approximately 10^{-3} S cm^{-1}) [107] when fabricated on Li surface at room temperature. [108] This remarkably simple compound has been known for over a century, but it is only within the last decade that the potential of the material and its derivatives has begun to be realized. [109] In an attempt to improve the behavior of Li electrodes as LIB electrode material, Li_3N was often used to modify the surface of Li electrodes. For example, Aurbach and his co-workers modified Li electrode by doping with Li_3N and reported a discharge capacity of 480 mAh/g after 108 charge-discharge cycles. [110] Wu *et al*. also compared the electrochemical behaviors of as-received Li electrode and Li_3N modified Li metal electrode at different exposure time to N_2. [107] The capacity retention of the 1h exposure N_2 time Li_3N modified Li metal electrode was about 20% higher than the as-received Li electrode. The enhanced performance of the Li_3N modified Li metal electrode was due to cycling efficiency of the lithium which depends on exposing time of the N_2. Other alkali and alkaline-earth metal nitrides were synthesized but are debatable due to their low thermodynamic stability. [111-113]

On the other hand, binary transition metal nitrides are of interest for replacing alkali and alkaline-earth metal nitrides in thin-film lithium-ion batteries [69, 105, 114] because of their low and flat potentials close to that of lithium metal along with high reversibility and large reversible capacities for lithium batteries.[106, 115] The pioneering work of transition metal nitrides was demonstrated by Bates *et al*. using Zn_3N_2 and Sn_3N_4 thin films as negative electrodes. [116] Tin nitride was reported with initial discharge capacity over 1100 $\mu Ah/cm^2$ and retaining about 520 $\mu Ah/cm^2$ capacity after 100 cycles. [117, 118] Also, stoichiometric germanium nitride also delivers a capacity of 500 mAh/g and maintaining good cycling stability above 400 mAh/g at a current density of 11.4 mA/g. [119] However, these metal nitrides were observed to exhibit low capacity due to low valences and oxidation states. Therefore, it is of interest to examine the electrochemical reactivity towards lithium of binary metal nitrides with high valences and oxidation states. Higher capacity values of about 1000 mAh/g have been found in some transition metal nitrides due to the high valence such as in chromium or vanadium nitrides with oxidation states of +3 [56, 120, 121] and molybdenum nitride with oxidation states of +2. [57] This is because they possess the advantages of corrosion resistance, high temperature and chemical stability. [122] Apart from transition metal nitrides, researches have been reported on nitrides of the platinum-group metals (Pt, Ir, Os, Ru, Rh, Pd), [123-125] Os nitrides,[126] and some nitrides thin films of group 5A and 6A. [82, 127] So much effort to achieve remarkable cyclability, stability and high-rate performance metal nitride electrodes for LIBs has been reported. However, metal nitride thin films were still unable to meet up with these characteristics. Additionally, their preparations are not cost effective and very tedious. The need for metal nitride electrode materials with cheaper and convenient preparation process that can accommodate large strains, reduce volume expansion and provide short diffusion pathway for Li^+ insertion and extraction were required.

An approach to solve such problems of binary metal nitride films is to fabricate nanostructure metal nitrides. Attentions were drawn to metal nitrides nanostructures due to their low cost, [68] environmental friendliness, [68, 128] ability to accommodate large strains, decrease in huge volume changes and provision of short diffusion pathway for Li^+ insertion and extraction. [25, 128-133] Many metal oxide and carbon based electrodes have been reported for nanostructure materials and great achievements have been made. [7, 25, 134-137] However, few reports can be accounted for nanostructure metal nitrides when compare to metal oxides and carbon based electrodes. [18] Nanostructure materials have also been discovered to overcome obstacles such as volume expansion and poor diffusion pathway in metal nitride electrodes. [83] The development of metal nitrides nanomaterial starts to gain attention as Chowdari and his Co-workers reported the prime metal nitride nanomaterial, cobalt nitride (CoN) nanoflakes. [83] CoN nanoflake delivers a capacity of 990 and 690 mAh/g at 0.33 C and 6.6 C after 50 and 80 cycles respectively. The most interesting thing was that the discharge capacity of the nanoflaky CoN increases with increasing cycling even at high current rate of 6.6 C. Reddy and his co-workers compare the lithium storage performance of CoO, Co_3O_4 and CoN. [138] Among these cobalt compounds, CoN was reported to be the best anode material. It was figure out that the excellent performance of the CoN is due to the nitrogen that allows the formation of Li_3N and Co, resulting in an even higher theoretical capacity of 1100 mAh/g.

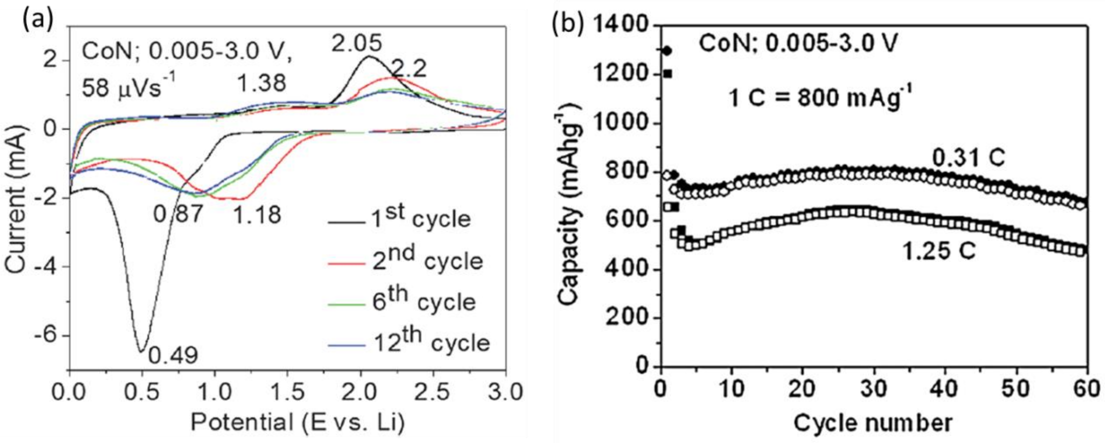

Figure 4. (a) Cyclic voltammograms of porous-CoN nanoparticles; 1–12 cycles. Selected cycles are given for clarity. Scan rate: 58 mV/s; the numbers represent cycle numbers. (b) Capacity vs. cycle number plot for porous-CoN nanoparticles at different current rates. Voltage range: 0.005–3.0 V. Closed symbols: discharge capacity; Open symbols: charge capacity. Reproduced from Ref. [139] with permission from The Royal Society of Chemistry.

Recently, Chowdari *et al*. studies CoN nanoparticles as high performance anode for LIBs. [139] During the first cycle, a strong cathodic peak was observed at 0.49 V (Figure 4a). In the subsequent cycles, the peak becomes broadened and shift to the high voltage region. As a result, the first discharge capacity was 1290 mAh/g which was higher than the theoretical capacity of CoN (1102 mAh/g). A capacity of 660 mAh/g and 470 mAh/g was retained after 60 cycles at a current rate of 0.31 C and 1.25 C respectively (Figure 4b). This result shows high reversibility and attractive cyclic performance that those of the lithiated cobalt nitride. [89, 90, 140] Besides CoN, other transition metal nitrides have been widely used anode for LIBs [59, 141, 142] due to their low cost, high molar density and superior chemical resistance. [8, 18] For example, CrN nanoparticles were studied by Chowdari *et al*. When the CrN was cycled at 0.1 C, the first-cycle reversible capacity of 635 mAh/g slowly decreases to 500 mAh/g after 10 cycles and remains stable up to the end of the 80th cycle. At 0.5 C, the CrN showed a stable capacity of 350 mAh/g for 40 cycles and the original capacity was regained when cycled at 0.1 C-rate. Gillot *et al*. demonstrated nanostructure nickel nitride electrochemical behavior against lithium which delivers a specific capacity of about 1200 mAh/g, [59] while titanium nitride nanowires were also reported to have an initial discharge capacity of 567 mAh/g and capacity retention of 455 mAh/g after 100 cycles. [142]

3.3. Metal nitrides composites for lithium storage

Lithiated metal nitrides and single metal nitrides have contributed immensely to the electrochemical properties of metal nitrides as electrodes for LIBs. Recently, metal nitride combine with other electrodes to form composites. Composites have been proved to contribute effectively to the conductivity and stability of LIB electrode materials. [143, 144] Metal nitrides have been widely applied to stabilize the poor stability and improve the electrical conductivity of other prominent electrodes. Transition metal nitrides such as TiN, was first used as composites to play the role of improving the conductivity and stability of other materials [145] because they were reported to possess good electrical conductivity, [146] extreme hardness, [147, 148] high melting temperature, [149] high chemical and thermal stability. [150] In this regard, transition metal nitride composites are considered to be the promising anode material in LIB for their high reversible reaction, high rate capability and good stability. [18] For instance, Kim and his co-workers reported the electrochemical properties of Si/TiN nanocomposites and TiN play as inactive material to maintain the stability of the nanocomposites. [145] Apart from utilizing TiN to maintain stability of nanocomposites, the metal nitrides also serve as protecting inactive material for electrode materials with more vacant sites that can accommodate metal nitrides. [151, 152] This has given $Li_4Ti_5O_{12}$ consideration because $Li_4Ti_5O_{12}$ suffers from poor electronic conductivity [153, 154] but consist of vacant sites that can accommodate metal nitrides. [155] For instance, DeSisto *et al*. prepare lithium titanate powder coated with TiN layer. [156] This composite delivers a capacity of 160 mAh/g over that of bare and unstable lithium titanate powder at 122 mAh/g. The result obtained shows an improved electronic conductivity. Park *et al*. also prepared $Li_4Ti_5O_{12}$/TiN nanocomposites by annealing $Li_4Ti_5O_{12}$ in flowing NH_3 gas. [157] Excellent discharge capacity of 120 mAh/g was delivered by the

$Li_4Ti_5O_{12}$/TiN composite at high current rate of 10 C after 70 cycles mainly due to the formation of amorphous TiN with metallic conductivity on the surface of $Li_4Ti_5O_{12}$.

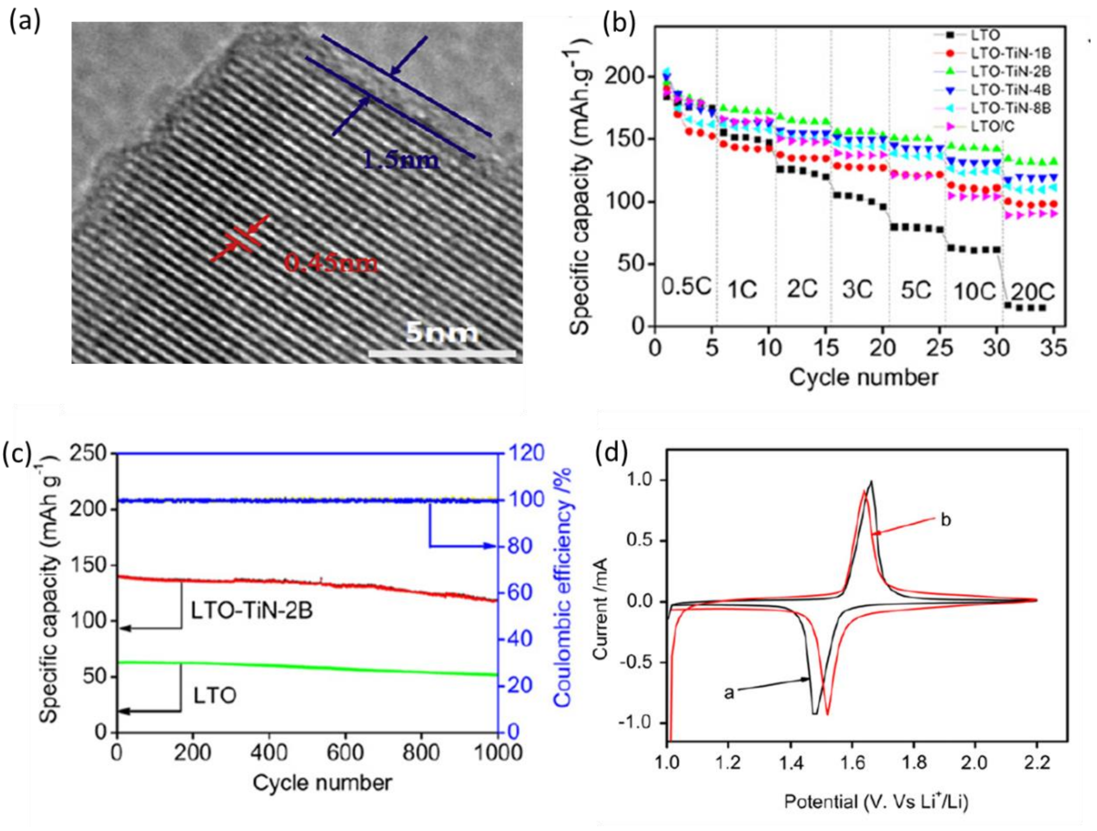

Figure 5. (a) High-resolution TEM image of LTO-TiN-2B. (b) Rate performance of high-energy ball-milling of $Li_4Ti_5O_{12}$/TiN. (c) Cyclic performance of pristine LTO and LTO-TiN-2B electrodes at 10C. (d) Cyclic voltammograms of pristine LTO and LTO-TiN-2B. Reproduced from Ref. [158] with permission from Elsevier.

Lately, $Li_4Ti_5O_{12}$ surface coated with TiN was reported by Zhang *et al*. (Figure 5).[158] As shown in Figure 5a, the high-resolution TEM displays the successful coating of the TiN on the $Li_4Ti_5O_{12}$ surface which allow easy lithium transportation enabling the composites to have a high capacity of 130 mAh/g at a charge/discharge rate of 20 C (Figure 5b). 85% capacity retention after 1000 cycles at 10 C was delivered (Figure

5c). The first reversible capacity of about 200 mAh/g and a redox peak at 1.45 V and 1.66 V confirms Li^+ insertion/extraction behavior of the $Li_4Ti_5O_{12}$ surface coated with TiN electrode (Figure 5d). Zhang's work displays excellent stability and rate capability as a result of improved conductivity concluding this electrode as great potential as an anode material for high-rate LIBs. [52] Enlightened by successful coating of metal nitrides on the surface of $Li_4Ti_5O_{12}$, many researches were reported base on partial nitridation of the metal oxides surfaces. This partial nitridation method could avoid the high temperature risk of annealing electrode materials in NH_3 gas to obtain metal nitrides. For example, TiO_2 was slightly nitrided in NH_3 gas to obtain nitridated TiO_2. [159] The nitridated TiO_2 delivers a discharge capacity of 156 mAh/g after 100 cycles at 0.2 C and about 50 mAh/g at high current rate of 10 C which doubles those of bare TiO_2 nanofibers at the same current rate. The improvement of the nitridated TiO_2 was mainly attributed to shorter lithium ion diffusion length and high electronic conductivity along the surface of nitridated hollow nanofibers. Also, Zheng *et al*. modified the surface of Fe_3O_4 nanoparticles with Fe_3N. [160] The Fe_3O_4@Fe_3N nanocomposites exhibited excellent electrochemical performance, such as a high reversible capacity over 739 and 620 mAh/g after each 60 cycles at a current density of 50 and 200 mA/g. The improvement was confirmed to be attributed to the Fe_3N coated layer, which could largely enhance the electronic conductivity and protect the Fe_3O_4 nanoparticles from the large variation of volume during the reaction with Li ions.

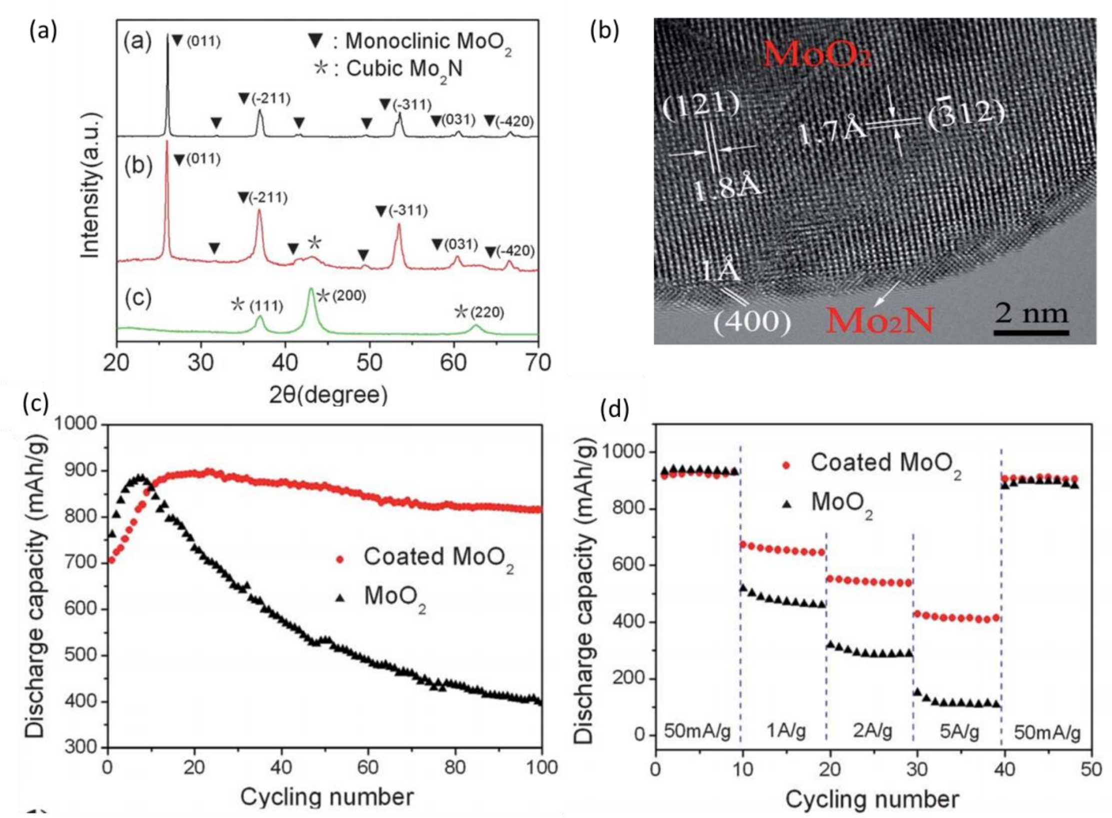

Figure 6. (a) XRD of the products obtained (b) HRTEM characterization of the Mo_2N nanolayer coated MoO_2 hollow nanostructures (b) The discharge capacity as a function of the cycle number for MoO_2 hollow nanostructures and Mo_2N nanolayer coated MoO_2 hollow nanostructures at a current density of 100 mA/g. (c) Rate capability of the samples up to 5000 mA/g. Reproduced from Ref. [150] with permission from The Royal Society of Chemistry.

Recently, Liu *et al*. reported that nanocoating of Mo_2N on the surface of MoO_2 is highly effective in improving the conductivity of MoO_2 over the bare MoO_2 (Figure 6). [150] The products in the first step (reduction of MoO_3 to MoO_2) were well indexed to a monoclinic cell with a=5.620(8) Å, b=4.868(2) Å and c=5.633(4) Å, confirming that the product obtained by reducing MoO_3 powders is MoO_2 with a monoclinic structure. In the nitridation to Mo_2N, (second step), the XRD patterns of the products show another wide peak, which also matched with a strong peak (200) of cubic Mo_2N (Figure 6a). The high-resolution TEM (HRTEM) image taken from the edge of an individual nitrided MoO_2 nanocrystals and subsequently displays how the Mo_2N was formed on the surface of the MoO_2 (Figure 6b). When these composites reacts with lithium, high specific capacity up to 815 mAh/g at more than 100 cycles were reported which doubled that of bare MoO_2 (Figure 6c). Very high-rate discharge capacity of 415 mAh/g at a current density of 5000 mA/g can also be observed in Figure 6d which is almost three times higher that than of MoO_2. Interestingly, such excellent electrochemical performance could be observed by the Mo_2N coated MoO_2 without the use of binder i.e. the Mo_2N coated MoO_2 electrode is a binder free electrode.

Binder free electrodes have attracted significant attention as a result of their ability to reduce the internal resistance that could lead to improved electrochemical performance of LIBs [161-164] Due to this intriguing advantage of the binder free materials, carbonaceous material such as graphene [165, 166] entice researchers because carbonaceous materials are binder free which also have high electrical conductivity. [167-169] Combination of such binder free materials and metal nitrides have been proved to contribute positively to the conductivity of metal nitrides [170] For instance, Zhang's paper reported VN and graphene composite with an initial coulombic efficiency of 74.6% which is higher than of the pristine VN at 55.8%. [171] An increasing in discharge capacity up to 983 mAh/g after 175 cycles was observed due to the fact that there is a strong synergistic effect between VN and G after considerable cycles. VN was mixed with graphene in order to simultaneously improve the electronic conductivity and the coulombic efficiency of the composites.

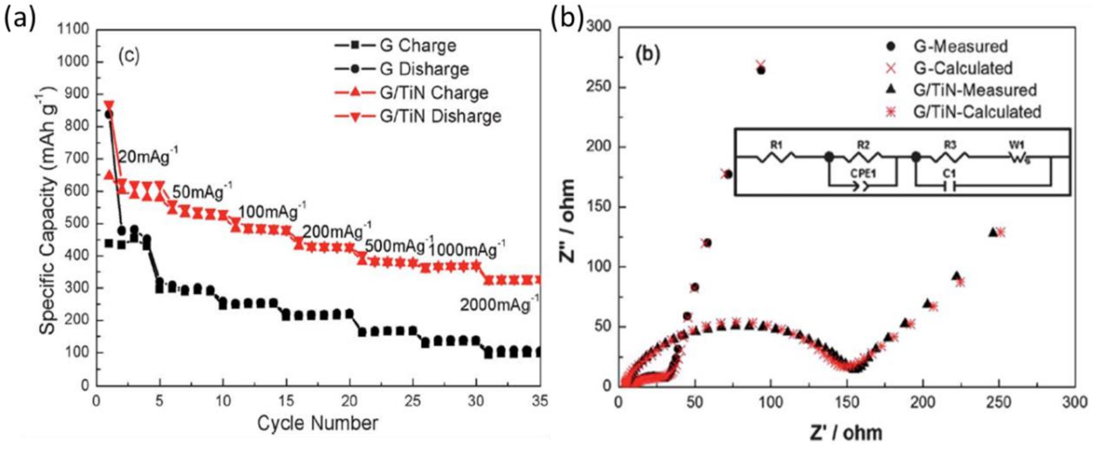

Figure 7. (a) Rate performance of G/TiN and G. (b) Nyquist plots for G/TiN and G at 3.0 V (vs Li^{+}/Li) after 3 cycles and corresponding simulation results (inset is the equivalent circuit used to fit an experimental curve). Reproduced from Ref. [172] with permission from The Royal Society of Chemistry.

Also similar work was carried out by Yue *et al*. in an in-situ synthesis of a binder free graphene/titanium nitride (G/TiN) hybrid material as shown in Figure 7. [172] An increase in the initial coulombic efficiency from 52% to 75% is acquired after TiN integration. The TEM carried out before and after cycling shows TiN nanoparticles display little change, as the lattice parameters are found to be identical before and after cycling which present considerable defects, possibly from the incorporation of N during material synthesis, which could partially be responsible for the enhanced property. The G/TiN hybrid anode accounts for a reversible capacity as high as 325 mAh/g at 2000 mA/g much higher than that of pure graphene at 98 mAh/g after about 35 cycles (Figure 7a). Their electrochemical impedance spectroscopy result justifies that an enhanced electronic conductivity was observed due to the addition of TiN (Figure 7b), indicating that the integration of TiN on G is beneficial for the formation of a favorable solid electroloye interface (SEI) layer and charge transfer resistance. The SEI layer is the layer formed when electrolyte decomposes during the discharge process of an electrode material in LIB. Electrolyte decomposition in the graphene/TiN could lead to the formation of some products, which might be responsible for the excellent electrochemical performance of the G/TiN composites over the bare graphene electrode. This demonstrates that metal nitrides hybrids display a superior electrochemical performance owing to the highly efficient mixed (electron and Li^+) conducting network. For proper clarification of these nitrides electrochemical performances, we summarized the result of some reported works in the Table 1. Table 1 analyses the theoretical capacity (TC) and experimental capacity (EC) of some metal nitrides that has been used as electrode materials in LIBs. The TC of metal nitrides composites are based on the TC of the core material. For example, in $Li_4Ti_5O_{12}$@TiN composite, the TC is 175mAh/g which is the TC of $Li_4Ti_5O_{12}$.

In recent years, flexible electronics are emerging and promising technology for next-generation, high-performance portable electronic devices. [173, 174] They require the development of thin, lightweight, and flexible energy-supply devices such as LIBs and SCs. [175] Future demand necessitates the development of advanced electrode materials with high capacity, rate capability, cycling stability, electrical conductivity and mechanical flexibility. [176] In recent years, lots of flexible full LIBs based on CNT, [177] cellulose paper, [178] graphene, [179] metal oxides, [180], [161] binary metal oxides; [181]; and metal sulfides [182] have been reported. Flexible devices based on metal nitrides are rarely reported. [186] The metal nitrides possess interesting mechanical properties such as high hardness, contradictory ductile vs. brittle behavior and the presence of vacancies on the metal and anion sites in their components, which make them suitable for application in flexible devices. [183, 184]

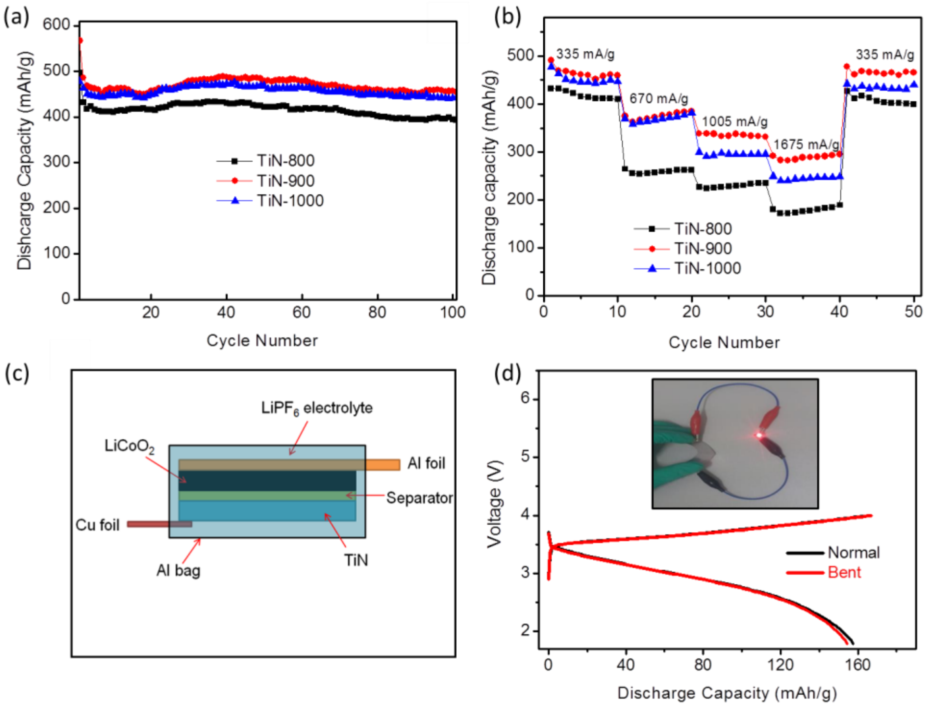

Figure 8. (a) Cycle performance of TiN electrodes at a voltage range of 0.01–3V (vs. Li^+/Li) for 100 cycles. (b) Rate capability measurements of the TiN electrodes at different current densities. (c) Schematic structure of a flexible Li-ion battery. (d) Charge-discharge curves of $LiCoO_2$//TiN-900 at the normal and bent position after the 5th and 10th cycle respectively. Inset is the demonstration of the $LiCoO_2$//TiN-900 full battery powering a red LED at the bending position. Reproduced from Ref. [142] with permission from The Royal Society of Chemistry.

Until recently, Lu *et al*. demonstrated the first metal nitride based anode flexible LIBs (Figure 8). [142] The flexible TiN nanowires were first study as anode for LIB in a half-cell and high initial discharge capacity of 567 mAh/g was reported (Figure 8a). The flexible TiN anode retains 80% of the initial capacity after 100 electrochemical cycles. Also, at a high current density of 1675 mA/g, it could deliver a capacity of 288 mAh/g (Figure 8b). The flexible TiN nanowire was then used as an anode material in the fabrication of a flexible full LIB. Figure 8c show the graphical structure of the flexible LIBs with the flexible TiN as anode, $LiCoO_2$ as cathode, $LiPF_6$ electrolyte and a separator. The initial discharge capacity of the battery is 167 mAh/g at the normal position with capacity retention of 95% after 120 cycles. The charge/discharge curves plotted for the $LiCoO_2$//TiN-900 full battery at the normal position and bent position were very similar (Figure 8d). The impedance of the battery at the normal and bent position is almost the same when EIS measurements was performed which verifies that the bending has no negative effect on the resistance of the battery. This flexible full LIB could power a red light-emitting diode (LED) when bent as displayed in the inset of figure 8d.

Table 1. A summarization of the Initial capacity and discharge capacity of different metal nitride electrode materials in LIBs

Types of Metal Nitrides	Different Metal Nitride Electrode Materials	Initial Capacity (mAh/g)	Discharge Capacity (mAh/g)
Lithiated Nitrides	Li_7MnN_4	250 at 1 C	240 after 50 cycles
	$LiMoN_2$ [54]	110 at 2 mV/g	110 after 1 cycle
	$Li_{2.6}Co_{0.2}Cu_{0.15}Fe_{0.05}N$[93]	781 at 0.15 mA/cm^2	700 after 60 cycles
	$Li_{2.7}Fe_{0.3}N$[86]	550 at 0.16 mA/cm^2	550 after 1 cycle
	$Li_{2.5}Co_{0.2}Cu_{0.1}Ni_{0.1}N$[93]	717 at 0.15 mA/cm^2	610 after 60 cycles
	$Li_{2.6}Co_{0.2}Cu_{0.2}N$	500 at 0.15 mA/cm^2	590 after 60 cycles
	$Li_{2.6}Co_{0.4}N$ [185]	1220 at 0.4 mA/cm^2	390 after 25 cycles
Ternary Nitrides	$Cr_{1-x}Fe_xN$ [58]	1800 at 0.028 mA/cm^2	750 after 30 cycles
Single nitrides	$SiN_{0.92}$ [82]	1800 at 0.2 C	1300 after 100 cycles
	VN [56]	1500 at 0.028 mA/cm^2	800 after 50 cycles
	CrN [120]	1800 at 0.028 mA/cm^2	1218 after 30 cycles
	Sb_3N [127]	748 at 0.02 mA/cm^2	825 after 50 cycles
	Zn_3N_2 [106]	1325 at 23 mA/g	555 after 1 cycle
	Ni_3N [59]	1200 at 1 Li at 20 h	500 after 10 cycles
	Fe_3N [69]	440 at 0.007 mA/cm^2	348 after 40 cycles
	Co_3N [69]	420 at 0.007 mA/cm^2	410 after 40 cycles
	CoN [83]	1080 at 0.33 C	990 after 80 cycles
	Mn_3N_2[70]	853 at 80 mA/g	463 after 110 cycles
	TiN [142]	567 at 335 mA/g	455 after 100 cycles
	Mo2N [57]	1226 at 0.1 mA/cm^2	696 after 100 cycles
Composite Nitrides	MoO_2@Mo_2N [150]	706 at 100 mA/g	815 after 100 cycles
	$Li_4Ti_5O_{12}$/TiN [157]	162 at 1 C	161 after 40 cycles
	G/TiN [172]	646 at 20 mA/g	554 after 200 cycles
	VN/GC [171]	300 at 21 mA/g	340 after 10 cycles
	TiVN/C [8]	1200 at 74.4 mA/g	678 after 20 cycles
	Si/TiN [145]	3000 at 0.23 mA/cm^2	300 after 20 cycles
	TiN@C [170]	157 at 50 mA/g	76 after 200 cycles

4. Metal Nitrides for Supercapacitors

The electrodes for SCs are the main question mark. Carbon materials, transition metal oxides and conducting polymers have been widely investigated as supercapacitor electrodes. Carbon-based materials such as carbon nanotubes, graphene possess prominent electrochemical stability and high electrical conductivity, but they suffer from low specific capacitance (90 to 250 F/g), which make them very challenging to develop high energy density SCs. [186] On the other hand, metal oxides and conducting polymers can deliver substantially higher specific capacitances of 300-1200 F/g through Faradaic reactions. However, their poor conductivity and general kinetically irreversibility limit their practical application for high energy density SCs. [27, 187, 188]

Metal nitrides have hold increasing attention as SCs electrodes since they have significant advantages. Firstly, they have excellent much superior electrical conductivity (4000 -55500 S/cm) than most of metal oxides, and thus exhibiting higher power density. [189, 190] Secondly, the capacitances of the metal nitrides are substantially larger than the carbon materials and comparable to most of the metal oxides, which give rise to their high energy density. [189, 191] Third, they also possess high mechanical stability than the metal oxides. [192-195] Such these features make them very promising as high-performance electrodes in SCs.

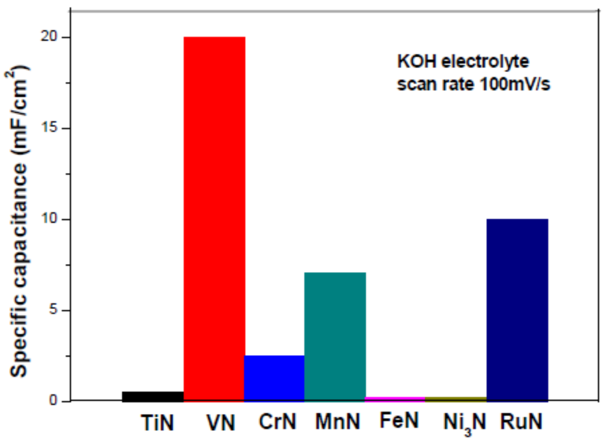

Figure 9. Specific capacitance of transition metal nitride thin films. Reprinted with permission from Abstract #494, Honolulu PRiME 2012, © 2012 The Electrochemical Society

Many research works have demonstrated the use of various transition metal nitrides in SCs. [196] Bouhtiyya *et al*. Summarzes the performance of different metal nitrides, using KOH electrolyte solution. These nitrides have shown a capacitive behavior at high scan rates due to their high electronic conductivity and fast reversible redox process (Figure 9). [47] Apart from the commonly reported metal nitrides, especially those metal nitrides in Figure 9, some other nitrides such as niobium nitride (NbN), tungsten nitride (WN) and tantalum nitride (Ta_3N_5). [60, 61] Choi and Kumta reported that, after 500 cycles in 1 M KOH solution, NbN could retain a capacitance of 100% indicating no loss in the capacitance of NbN. [60] This was even better than Mo_2N that have already loss 40% after 500 cycles. Also, only 20% decrease in specific capacitance was observed for WN in 1M KOH electrolyte at a scan rate of 50 mV/s. [61] The next subsection will deeply discussed, details about the development of

Mo_2N, TiN and VN as SC electrode materials, as part of the most commonly reported SC electrodes based on metal nitrides.

4.1. Molybdenum Nitrides Based SCs

Among the transition metal nitrides, molybdenum nitrides were the first metal nitride to be reported as SC electrode materials. [197] Conway and his co-workers considered the high cost of RuO_2 and evaluated Mo_2N and MoN as possible substitutes for RuO_2. The films of molybdenum nitrides exhibit quite similar capacitative behavior to that of RuO_2. Li *et al*. synthesized Mo_2N nanoparticles and studied their electrochemical performance as SCs electrode. [198] The as-prepared γ-Mo_2N nanoparticles showed good electrochemical performance with a high specific capacitance of 172 F/g and a broadened potential window ranging from -0.6 V to 0.5 V in 1 mol/L H_2SO_4 electrolyte. Also, Kherani et al. shows that Mo_2N shows a specific capacitance of 16 mF/cm^2 which is 200 times higher than its corresponding oxide (0.67 mF/cm^2) when cycled in 0.5 M H_2SO_4 electrolyte solution at a scan rate of 50 mV/s. [199] The excellent performance of the Mo_2N over the MoO_2 was attributed to the pseudocapacitive effect of Mo nitride. After nitridation, the Mo film also exhibited enhanced stability in acidic environment compared to the as-deposited Mo oxide film. An important difference between the nitride films and RuO_2 is that the potential range of reversible capacitative behavior is only over ca. 0.6 V, unlike RuO_2 for which the range is Ca. 1.4 V. Beyond the range of 0.6 V in the positive direction, decomposition or some dissolution of the nitride films takes place. The potential range of capacitance behavior is an important factor for practical supercapacitor development and ideally, it should be limited only by the voltage window of the electrolyte solution. This places a severe limitation on the usefulness of MoN or Mo_2N films as substitutes for RuO_2 in redox-pseudocapacitance types of capacitor devices. In an attempt to increase the potential range of molybdenum nitrides, Wang *et al*. reported that the addition of tantalum oxide on molybdenum nitride with potential window of -0.2 – 0.85 V. [200] Such potential window was higher than those reported from some other molybdenum nitride but still unable to reach that of RuO_2 at 1.4 V. [198, 201] Contemplating on the issue of increasing the potential range of molybdenum nitrides, increasing the capacitance of molybdenum nitride remains a vital challenge. Molybdenum nitride combined with other compounds and some improved capacitance was recorded. [202-204] In Wang's work, composite of Mo_2N/Co_3Mo_3N provides specific capacitance of 109.9 F/g [205] and specific capacitance of 105.83 F/g for tantalum oxide and Molybdenum nitride composites [200] while the pristine Mo_2N could only delivered 30 F/g at a scan rate of 100 mV/s.

4.2. Titanium Nitride Based SCs

Compare to Mo_2N, titanium nitride (TiN) has attracted great interests for SCs [206] because of its superior electrical conductivity (4000−55500 S/cm) [207] and mechanical stability. [208] For instance, Kherani's group recorded a specific capacitance of 0.067 mF/cm^2 for TiN in H_2SO_4 electrolyte solution at 50 mV/s [199] and Sun *et al*. also fabricated TiN nanorods by an electrospinning method. [209] The TiN nanorods showed a specific capacitance of 38.5 F/g at a current density of 40 mA/g in KOH electrolyte. Cui's group prepared mesoporous TiN microspheres with 144 F/g at 50 mA/g in

$LiPF_6$ electrolyte solution [210] likewise the specific capacitance evaluated by cyclic voltammetry in 1 M KOH electrolyte was 238 F/g at 2 mV/s for nanocrystalline TiN. [211] However, the application of TiN electrodes is greatly limited by their poor stability. [210, 212]

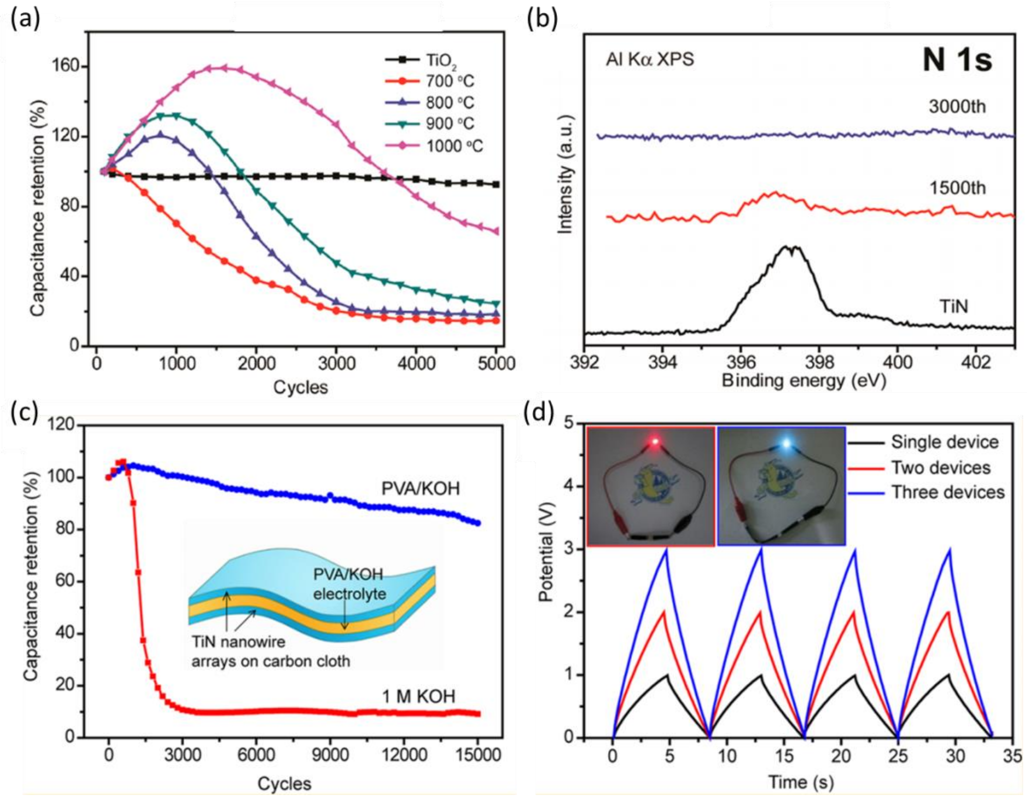

Figure 10. (a) Cycle performance of TiO_2 and TiN electrodes collected at a scan rate of 100 mV/s for 5000 cycles. (b) Core level N 1s spectra collected for the TiN-800 electrode at different cycles. (c) Cycling performance collected at a scan rate of 100 mV/s for the TiN-SC with PVA/KOH polymer electrolyte and in a 1 M KOH aqueous electrolyte. (d) Galvanostatic charge/discharge curves collected at a current density of 4 mA/cm^2 for a single solid-state TiN-SC and tandem devices where two and three SC units are connected in series. Inset: red and blue LEDs were powered by the tandem

TiN-SCs. Reproduced from Ref. {Lu, 2012 #6} with permission from American Chemical Society.

To understand the electrochemical instability of TiN nanostructures, Lu *et al.* use TiN nanowires as an example to elucidate the mechanism causing the capacitance loss. {Lu, 2012 #6} They systematically studied the modifications of morphology, chemical composition, and electrical conductivity of flexible TiN nanowire electrode during the cycling process, and revealed that the irreversible electrochemical oxidation reactions and structural pulverization are the main reasons for the electrochemical instability of TiN electrodes (Figure 10). Figure 10a demonstrates cyclic performance of TiN at different temperatures up to 5000 cycles. The specific capacitances of TiN electrodes increase gradually in the first 1000−2000 cycles due to self-activation process and then suffer from drastic loss of capacitance. The capacitance retentions for the TiN-800, TiN- 900, and TiN-1000 samples at 5000 cycles are measured to be 18.6%, 24.5%, and 65.8%, respectively (Figure 10a) but still higher than some other early reports.[209-211] It is clear that substantial improvement of TiN electrochemical stability is essential for practical application. To understand the origin of the instability of TiN NWs, the chemical composition during the cycling test was studied. Figure10b shows N1s XPS spectrum collected for the TiN-800 electrode at different cycles. The nitride and oxynitride N 1s XPS peaks decrease gradually and consequently disappear after 3000 cycles. This indicates that the instability of TiN electrode is due to irreversible electrochemical oxidation reaction in aqueous solution. Solid-state polymer electrolyte was then used to enhance the stability of the TiN nanowires. The electrochemical stability of the TiN-SCs was examined at a scan rate of 100 mV/s and the TiN electrode shows greatly improved stability with an extremely high capacitance retention of 82% after 15 000 cycles (Figure 10c), compared to the same TiN electrode tested in 1 M KOH electrolyte solution. To demonstrate the potential use of these flexible solid-state TiN-SCs, supercapacitor units in series to drive light-emitting-diodes (LED) were connected. The electrochemical performances of the tandem TiN-SCs (two or three devices connected in series) were evaluated by charge/discharge measurements (Figure 4f). These tandem devices exhibit an enhanced potential window, which can power red and blue LEDs that have the lowest working potential of 1.5 and 2.5 V, respectively (Figure 4f inset).

Recently, Lu *et al*. further extended this work by using a thin carbon shell to improve the cyclic stability and capacitive performance of metal nitrides in solution-based electrolyte (Figure 11). [191] Carbon coating have been reported not only to improve the conductivity of electrode materials for energy storage devices but can also improve the stability. [213-216] Figure 11a shows the HRTEM of the composites which confirms the successful coating of the thin carbon shell on the surface of the TiN. The TiN@C electrode achieved a specific capacitance of 124.5 F/g at 5 A/g, which was higher than the TiN (107 F/g) and C (17.3 F/g) electrodes (Figure 11b).The TiN@C sample had a better capacitance rate capability. It retained more than 78.3% of its initial capacitance when the current density was increased from 0.25 to 5 A/g, while the retention rate was 70.2% for the TiN sample. More importantly, the TiN@C electrode exhibited a remarkable long-term stability, with 91.7% of its initial capacitance retained after 15 000 cycles as compared to 9.1 % for TiN electrode (Figure 11c). This value was even higher than the values obtained for the TiN electrodes (82%) in solid-state devices {Lu, 2012 #6} and is the best cycling stability ever achieved for TiN materials and for other metal–nitride materials. These results proved that the deposition of the ultrathin uniform carbon shell can effectively improve the capacitance and stability of TiN. Likewise, this method can also improve the electrochemical stability of other metal nitride electrodes for SCs. After coated a thin carbon shell, the VN@C electrode retained more than 88.4% of its initial capacitance after 15000 cycles (Figure 11d), which are substantially higher than that of the VN nanowire electrode (8.5%) and the other previously reported VN nanostructures. [217, 218] Such significant improvements in capacitive performance and stability are due to the fact that the ultrathin carbon shell not only effectively suppresses the electrochemical oxidation of the TiN NWs and retains their electrical conductivity, but it also preserves their morphology.

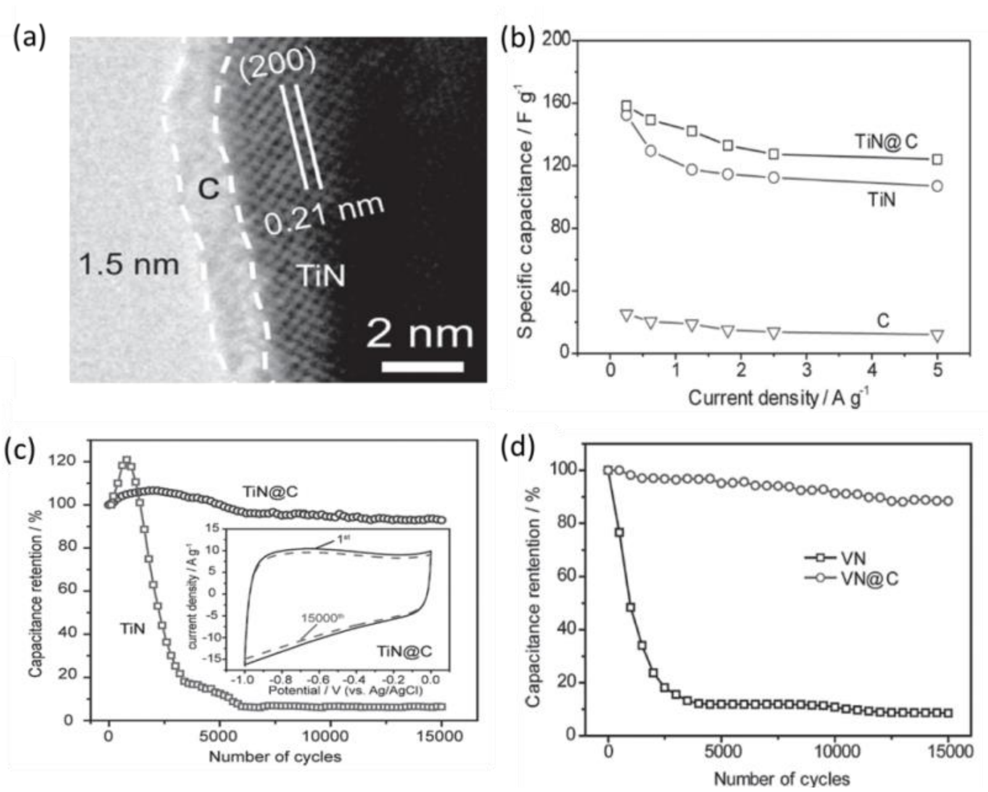

Figure 11. (a) HRTEM image showing the area indicated by the white rectangle. (b) Calculated specific capacitances (based on the discharge curves) of the electrodes plotted as a function of current density. (c) Cycling performance of the TiN (squares) and TiN@C (circles) NW electrodes, collected in 1 M KOH solution at a scan rate of 100mV/s for 15 000 cycles. Inset: The first and 15 000th CV curves collected for the TiN@C NW electrode. (d) Cycling performance of the VN and VN@C NW electrode collected in 1 M KOH solution at a scan rate of 100 mV/s for 15 000 cycles. Reproduced from Ref. [191] with permission from WILEY-VCH Verlag GmbH & Co. KGaA, Weinheim.

Improving both the capacitance and conductivity of metal nitrides as electrode material for SCs still demand much attention. Metal nitrides composites were considered by many researchers as a strategy to improve the capacitance and electronic conductivity simultaneously. Thus, they combine with other materials such as conducting polymers, [219] carbonaceous materials [220] and metal oxides [221] in order to improve or maintain stability and enhance rapid electron transportation in the electrodes. Among the materials metal nitrides often composite with, conducting polymers were coated on the surface of metal nitrides due to the ease of preparation and good environmental stability combined with moderate electrical conductivity. [222] This is to avoid the cycling degradation caused by volume changes and can also contribute to high pseudo-capacitance performance. [223] However, few studies were reported for conducting polymers and metal nitride composites. Qiu and Gao studied PANI/TiN composites and their results shows that the structure, morphology and electrochemical performance were controlled by the TiN, [224] another group recently demonstrated the PANI/TiN hybrid exhibits a capacity retention of 93% after 200 cycles in 1 M H_2SO_4 electrolyte solution. [225] The galvanostatic charge–discharge measurements of Ppy–TiN and Ppy–TiO_2 nanotube hybrids were also compared. [226] The Ppy–TiN has specific capacitance of 1265 F/g which is higher than that of Ppy–TiO_2 (382 F/g) at a current density of 0.6 A/g in 1 M electrolyte solution of H_2SO_4. Also, the Ppy–TiN composite exhibits stable capacitances of 459 F/g after 2000 cycles at a high current density of 15 A/g. The highly conductive titanium nitride substrate can promote the electrochemical capacitance of polypyrrole more significantly, as compared to the titania semiconductor, contributing to a higher supercapacitance performance of Ppy–TiN. Chu *et al.* studied a coaxial PANI/TiN/PANI nanotube arrays suitable for high-performance SCs in HCl electrolyte solution. [227] The nanocomposite electrode exhibits a high specific capacitance of 242 mF/cm^2 at a current density of 0.2 mA/ cm^2. After charging–discharging for 3000 cycles, 83% of the initial capacitance was retained.

Besides carbon coating and conducting polymers, the chemical stability of carbon nanotube (CNT), its high surface area and unique mesoporous network allow composite materials with higher capacitance and better cycle life to be obtained. [219, 228, 229] The electrical conductivities of TiN were improved by CNT in a study reported by Jiang *et al*. [230] As the content of CNTs increases, the surface area also increases and enhanced electrical conductivity of about 3.6 times from 144 to 516 S/cm was achieved. CNT–TiN nanocomposites were also fabricated by Jiang and Gao with enhanced electrical properties. [229] In the presence of 12 vol% CNTs, the CNT–TiN composite exhibits a 45% increase in electrical conductivity over that of the TiN material. The addition of CNTs still retains the original electrochemical stability of TiN after cycling. Another approach that has been used to achieve high capacitance for metal nitride is combining metal nitride with some higher energy density materials. For example, MnO_2/TiN heterogeneous nanostructure has been designed for energy storage in SCs which delivers a specific capacitance of 662 F/g at 45 A/g in 1 M HCl aqueous solution, [231] $Ni_xCo_{2x}(OH)_{6x}$/TiN electrode exhibits superior pseudocapacitive performance with a high specific capacitance of 2543 F/g at 5 mV/s, remarkable rate performance of 660 F/g at 500 mV/s, and promising cycle performance with about 6.25% capacitance loss for 5000 cycles in 0.1 M KOH and 1.9 M KCl aqueous solution. [232]

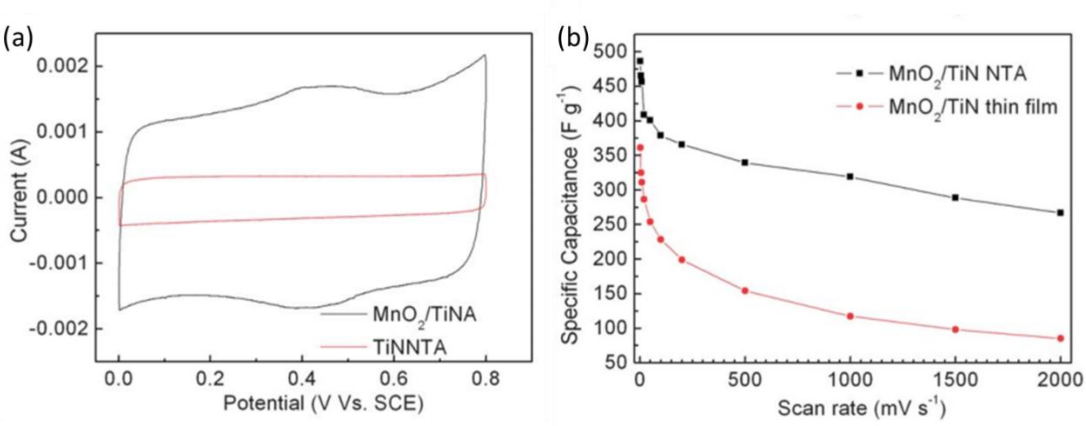

Figure 12. (a) Cyclic voltammograms of TiN NTA before (red) and after (black) the deposition of MnO_2 at 0.7 V for 10 s with a scan rate of 200 mV/s, (b) The specific capacitance (F/g) obtained from MnO_2/TiN NTA electrodes (black) and MnO_2/TiN thin film electrodes (based on the mass of MnO_2) as a function of scan rates. Reproduced from Ref. [221] with permission from The Royal Society of Chemistry.

The same group also displays one dimensional MnO_2/TiN nanotube coaxial arrays as high performance electrochemical capacitive energy storage (Figure 12). [221] Figure 12a shows the enclosed area of the CV curve, which was used to estimate the capacitance and is more than 4-fold larger after the deposition of MnO_2. The rate capability of this nanostructured electrode was remarkable, as it maintains a nearly ideal capacitive CV shape with only small distortions even at a very high scan rate of 2000 mV/s. This result in only a 45% loss of capacitance compared with that one measured at 2 mV/s (Figure 12c). Nyquist plot of the MnO_2/TiN nanotube coaxial arrays suggests that the nanostructured current collector provides an increased contact area with the active materials, and also enhances the electronic conductivity of the electrode. This research work figure out that the highly conductive and mechanically stable TiN greatly enhances the flow of electrons to the MnO_2 material, with improving high power combining the favorable structural, electrical and energy properties of MnO_2 and TiN into one system which allows for a promising electrode material for SCs. Base on the development of TiN as electrode material for SCs, the specific capacitance and rate capability delivered by some of the TiN electrodes were outline in Table 2, as well as the electrolyte solution selected for the electrochemical measurements.

Table 2. Summary of TiN and TiN composite electrodes according to the electrolyte solution, specific capacitance and rate capability

TiN Electrodes	Electrolyte Solution	Specific Capacitance	Rate Capability Capacitance
	Single Electrodes		
TiN Nanorods [209]	1 M KOH	38.5 F/g at 0.04 A/g	7.5 F/g at 0.64 A/g
TiN Microspheres [210]	1 M $LiPF_6$ (EC:DEC=1:1)	144 F/g at 0.05 A/g	39.4 F/g at 1 A/g
Nanocrystalline TiN [211]	1 M KOH	238 F/g at 2 mV/s	50 F/g at 100 mV/s
TiN Nanowires {Lu, 2012 #6}	PVA/KOH polymer gel	155 F/g at 0.25 A/g	117.5 F/g at 5 A/g
Porous TiO_xN_y [233]	2 M H_2SO_4	120.9 F/g at 1.25 A/g	55 F/g at at 3.75 A/g
Nitridated TiO_2 Sphere [234]	1 M H_2SO_4	1.9 mF/cm^2 at 0.005 mA/cm^2	1.4 mF/cm^2 at 1 mA/cm^2
	Composite Electrodes		
TiN/MnO_2 nanotubes [212]	1 A/g	853.3 F/g	150 F/g 15 A/g
TiN@C Nanowires [191]	1 M KOH	159.9 F/g at 0.25 A/g	124.5 F/g at 5 A/g
PANI/TiN[225]	1 M H_2SO_4	1066 F/g at 1 A/g	864 F/g at 10 A/g
PPy/TiN[226]	1 M H_2SO_4	1265 F/g at 0.6 A/g	459 F/g at 15 A/g
PANI/TiN/PANI[227]	1 M HCl	242 mF/cm^2 at 0.2 mA/cm^2	167 mF/cm^2 at 10 mA/cm^2
MnO_2/TiN nanotubes [231]	1 M $LiClO_4$	850 F/g at 0.5 A/g	662 F/g at 45 A/g
$TiN/Ni_xCo_{2x}(OH)_{6x}$ [232]	0.1 M-KOH 1.9 KCl	2580 F/g at 5 mV/s	1665 F/g at 100 mV/s
MnO2/TiN Nanotubes [221]	1 M Na_2SO_4	681 F/g at 2 A/g	267.2 F/g at 2000 mV/s
TN/VN Composites [55]	1 M KOH	170 F/g at 2 mV/s	74.46 F/g at 200 mV/s
TiN/VN Fibers [235]	1 M KOH	247.5 F/g at 2 mV/s	160.8 F/g at 50 mV/s

4.3. Vanadium Nitride Based SCs

Among the metal nitrides, vanadium nitride (VN) is emerging as the most attractive candidate as electrode material for SCs due to its ultrahigh specific capacitance of 1340 F/g and high electrical conductivity ($\sigma_{bulk} = 1.67 \times 106\ \Omega^{-1}\ m^{-1}$). Earlier, Choi *et al.* synthesizes chemically nanostructured VN for pseudocapacitor application and reported that the low-temperature synthesized nitrides exhibited the smallest crystallite size (≈ 6.3 nm) and high specific capacitance of 850 F/g at a current rate of 50 mV/s. [194] High capacitance was obtained due to a pseudocapacitance contribution from the nitride because the specific surface area of the nitride is only 38 m^2/g.

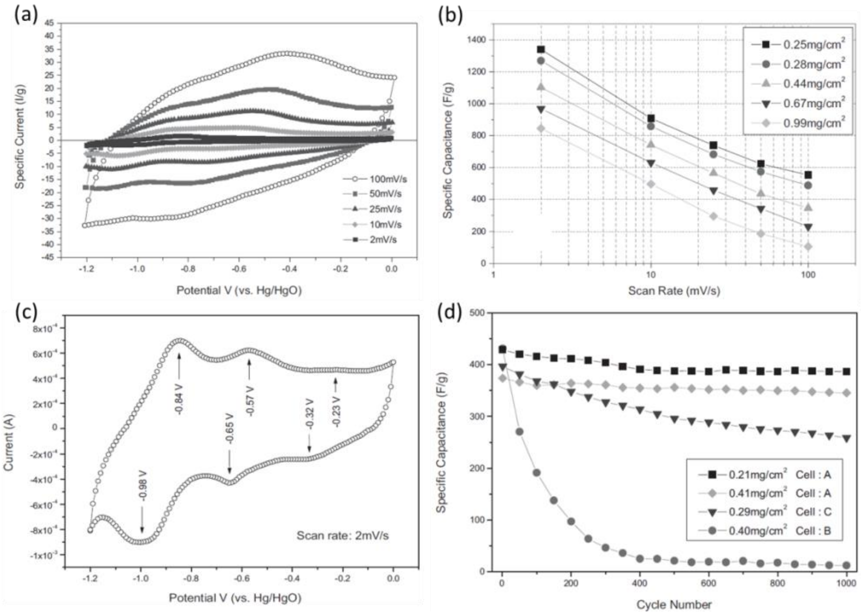

Figure 13. (a) CVs of VN nanocrystals synthesized at 400 ℃ at various scan rates (2–100 mV/s) in 1 M KOH electrolyte. (b) Specific capacitance versus scan rate with different active-material loading. (c) CV of VN nanocrystals synthesized at 600 ^{o}C scanned at 2 mV/s in 1 M KOH electrolyte. (d) Cyclic behavior of VN nanocrystals

synthesized at 400 °C scanned at 50 mV/s up to 1000 cycles. Reproduced from Ref. [217] with permission from WILEY-VCH Verlag GmbH & Co. KGaA, Weinheim.

By increasing the scan rate, the same group also reports fast and reversible surface redox reaction in nanocrystalline vanadium nitride as displayed in Figure 13. [217] Figure 13a shows that the specific capacitance improves with reduced material loading, and the highest specific capacitance of 1340 F/g is recorded at a scan rate of 2 mV/s, which decreases to 554 F/g when tested at 100 mV/s. Also, at a high rate of about 2 V/s, an impressive specific capacitance of 190 F/g was obtained (Figure 13b). The impressive specific capacitance which exceeds that of ruthenium oxides, has never been observed in transition metal nitrides, and indicates their possible use in electrochemical devices desirous of intermittent high pulse power. Figure 13c shows the charge mechanism of the VN crystals appears to arise from a combination of an electrical double-layer formation and the Faradaic redox reactions that occur on the surface of the partially oxidized nitride. As a result, it can be seen in Figure 13d that the VN nanocrystals can maintain a high specific capacitance (ca. 400 F/g) at a scan rate of 50 mV/s up to more than 1000 cycles without much loss (< 10%). The rate capability of the VN delivered by Choi's work still requires further improvement. With respect to different preparation methods and an effort to improve the electronic conductivity of VN, different VN were prepared. For example, VN powder was observed to have a capacitance of 161 F/g at 30 mV/s when synthesized by calcining V_2O_5 xerogel in a furnace under anhydrous NH_3 atmosphere at 400 °C as reported by Zhou et al. [193] Also, Glushenkov and his Co-workers reported that the capacitance of

186 F/g for VN in 1 M KOH electrolyte at 1 A/g in the structure and capacitive properties of porous nanocrystalline VN prepared by temperature-programmed ammonia reduction of V_2O_5. [218] Recently, Shu and his co-workers recorded an enhanced capacitance of 413 F/g at the current density of 1 A/g and 88 % of the maximum capacitance was retained when studied at a current load of 4 A/g which indicates an excellent rate capability of the nanocrystalline VN. [236] As the method of preparation has a lot to do with improved electrochemical performance of VN, thus we tabulated some of the result obtained for VN. Table 2 illustrates different syntheses of VN as reported by different groups including their specific capacitance, scan rates and voltage window.

Table 3. Specific capacitance, scan rates and voltage windows of VN with different synthesis method

Preparation Method	Specific Capacitance (F/g)	Scan Rate (mV/s)	Voltage Window (V)
Two-step ammonolysis Reaction	850	2	-1.2 - 0.0 [194]
	400	50	-1.2 - 0.0 [217]
Calcination	300	30	-1.1 - 0.0 [236]
	273	30	-1.1 - 0.0 [237]
	161	30	-0.95 - 0.15 [193]
Hydrothermal method	298.5	10	0.0 - 1.8[190]
Temperature programming	186	30	-1.2 - 0.0 [218]

Despite all these achievements, the application of vanadium nitride as SCs electrode was still limited due to poor cyclic stability and short cycle life. To improve such obstacles, Lu *et al*. studied the degradation mechanism of VN nanowires and utilizes LiCl/PVA polymer electrolyte to improve simultaneously the stability and the electronic conductivity of the VN nanowires (Figure 14). [190] The CV curves present essentially the same shape as the scan rate increases from 10 to 100 mV/s, indicating the good capacitive behavior of VN nanowires (Figure 14a). The VN nanowire electrode achieved an excellent specific capacitance of 298.5 F/g at the scan rate of 10 mV/s. The electrode exhibited remarkable cycling stability in LiCl/PVA gel electrolyte with a capacitance retention of 95.3% after 10 000 cycles while 14.1% capacitance was obtained in 5 M LiCl aqueous electrolyte (Figure 14b). Figure 14c shows the core level V 2p XPS spectra indicating why the VN nanowire electrode exhibits poor stability in aqeous electrolyte. This is as a result of VN oxidizing to VOx after cycling measurement. The VN nanowire electrode was employed as anode in asymmetric supercapacitors (ASCs). Figure 14d shows that the VN/VO$_x$ ASCs can operate up to a voltage of 1.8 V which is higher than that of RuO$_2$. The ASC device achieved a volumetric capacitance 1.35 F/cm^3 at current density of 0.5 mA/cm^2 with a remarkable rate capability, which retained about 74.7% of the initial capacitance (1.01 F/cm^3) as the scan rate increased from 0.5 to 5 mA/cm^2. The VO$_x$//VN-ASC device achieved a remarkable volumetric energy density of 0.61 mWh/cm^3 at current density of 0.5 mA/cm^2, which is 7 times higher than that of the VN-SSC device (0.079 mWh/cm^3).

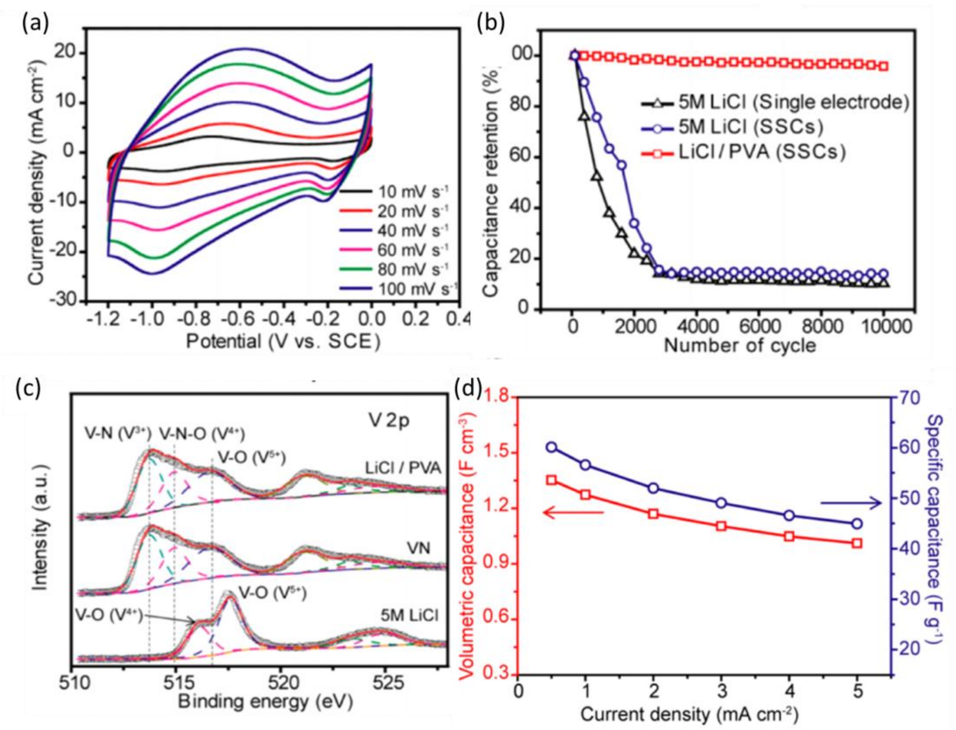

Figure 14. (a) CV curves and (b) Cycling performance of single VN electrode and symmetric VN SC devices collected at a scan rate of 100 mV/s for 10 000 cycles in 5 M LiCl aqueous electrolyte and LiCl/PVA gel electrolyte. (c) Core level V 2p XPS spectra collected for VN nanowires before and after testing for 10 000 cycles in LiCl aqueous electrolyte and LiCl/PVA gel electrolyte. (d) Volumetric capacitance and specific capacitance calculated for the VOx//VN-ASC device based on the galvanostatic charge−discharge curves as a function of current density. Reproduced from Ref. [190] with permission from American Chemical Society.

Owing to the improvement of the electrical conductivity of VN as electrode material for SCs, composites of VN were employed. For example, Ghimbeu and his co-workers demonstrate VN/CNTs composites. [238] The VN/CNTs composites delivered high capacitance retention (58%) at high current density (30 A/g) compared with just 7% of the pristine VN. The incorporation of CNTs during VN synthesis allows VN/CNTs nanocomposites with higher porosity, narrower pore size distribution, better conductivity and improved electrochemical properties to be obtained. Furthermore, Zhang *et al*. [239] reported high rate SCs from three-dimensional arrays of vanadium nitride functionalized carbon nanotubes (VN/GC) which demonstrated a respectable specific capacitance of 289 F/g in 1M KOH electrolyte at a scan rate of 20 mV/s, a superb rate capability at a very high scan rate of 1000 mV/s. They adopted a simple methodology to developed multiwalled carbon nanotubes conformally covered by nanocrystalline vanadium nitride. Such composites of VN were used to fabricate flexible SCs. A typical example is the work of Zhang *et al*. [240] Zhang *et al*. demonstrated spherical porous VN and NiO_x as electrode materials for asymmetric supercapacitor. The VN/NiOx asymmetric supercapacitor shows a sloping voltage profile from 0.5 to 1.45 V with excellent reversibility and delivers a specific capacitance of 139 F/g and excellent rate capability. It also displays a good cycling behavior with about 15% specific capacitance decay after 1000 cycles with specific energy 26 Wh/kg. Zhou's group fabricates flexible freestanding mesoporous VN nanowires (MVNNs)/CNT SCs and the electrochemical performance of the single electrode and hybrid symmetric supercapacitors (SSCs) were displayed in Figure 15. [241] The cyclic voltammetry (CV) curve shown in Figure 15a indicated that the capacitance of MVNN electrode was much larger than CNT and MVNN electrode. The areal capacitance of the freestanding MVNN/ CNT hybrid films in Figure 15b was 178 mF/cm^2 at a discharge current density of 1.1 mA/cm^2. The result obtained in further study of the MVNN/CNT electrode in SSC was highly attractive. The CV curves of the MVNN/CNT SSCs were almost rectangular shape between 0–0.7 V with scan rates varied from 5 mV/s to 100 mV/s (Figure 15c). Furthermore, galvanostatic charge/discharge curves indicated the charging curves were almost symmetrical. The volumetric capacitance was 7.9 F/cm^3 at 0.025 A/cm^3 and remained at 4 F/cm^3 at 0.5 A/cm^3. The energy and power densities were calculated to be 0.54 mWh/cm^3 and 0.4 W/cm^3 repspectively. The capacitance remained 82% of the initial capacitance at a current density of 0.2 A/cm^3 after 10000 charge-discharge cycles as shown in Figure 15d.

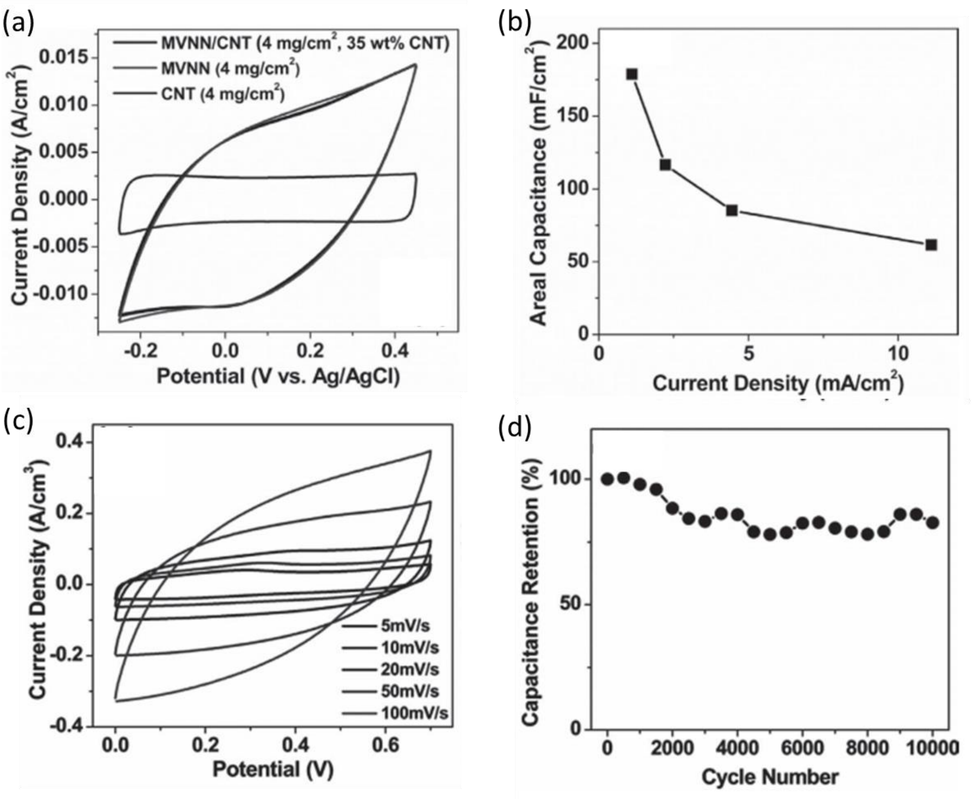

Figure 15. (a) CV curves of CNT electrode, MVNN electrode and MVNN/CNT hybrid electrode (35 wt% CNT) under the same mass loading by a typical three-electrode configuration. (b) Areal capacitance as a function of current density. (c) CV scan curves of the MVNN/CNT hybrid SSC. (d) Cycle life of the

MVNN/CNT hybrid SSC. Reproduced from Ref. [241] with permission from WILEY-VCH Verlag GmbH & Co. KGaA, Weinheim.

In addition, with the enthusiastic development of TiN and VN as SC electrode materials, combination of higher specific capacitance of VN and better rate capability of TiN named ternary nitrides have attracted the interest of many researchers but few developments have been made. Ternary nitrides are nitrides with two metal nitrides combined to form a composite. Dong and his Co-workers synthesizes TiN/VN composites and they reported that these composites deliver a specific capacitance of 170 F/g. [55] They attributed their excellent result to both vanadium and titanium nitrides having same diffraction patterns and similar cell parameters which allows fast transportation of electrons and hence, exhibits excellent storage performance. Also, mesoporous coaxial titanium nitride-vanadium nitride fibers of core/shell structures for high-performance SCs were reported by Zhou *et al.* [235]. These hybrids exhibited higher specific capacitance of 247.5 F/g at 2 mV/s and better rate capability 160.8 F/g at 50 mV/s. They related their higher specific capacitance and better rate capability to the mesoporous structure with unique dimensional structure and higher surface-area in the high electronic conducting transition nitride hybrids, which combined higher specific capacitance of VN and better rate capability of TiN.

5. Conclusion and Outlook

Contemplating on the issue of selecting efficient electrode material for energy storage devices, different electrode materials such as metal oxides, conducting polymers, carbonaceous materials have been discussed. Recently, metal nitrides have successfully gain an upper hand recently in LIBs and SCs due to their interesting morphology, high energy density, corrosion resistance and better cyclic characteristics. In this review, we summarize the progress of metal nitride as promising electrode material for LIBs and SCs. As for LIBs, different types of metal nitrides categorized by their nitride position have been reviewed with an emphasis on how these positions have affected their lithium storage performance positively. Base on the mostly reported metal nitride, we also discussed the development of metal nitrides as SC electrodes. Moreover, the development of metal nitrides in flexible energy storage devices has also been epitomized. Additionally, challenges facing metal nitrides as energy storage devices for LIBs and SCs were discussed and ways to developed them were also summarized.

Absolutely, electrode materials would involve series of complex chemical and physical procedures at the interface of electrode/electrolyte during the charge and discharge process. During this process, electrode materials face different difficulties such as volume expansion, poor conductivity, poor stability, stacking and so on. All these difficulties lead to poor electrochemical performance of the electrode materials for energy storage devices. Despite the fact that lots of achievements have been made on metal nitrides and these achievements have been discussed in this review, there exists substantial room for the development of more metal nitrides with excellent electrochemical performance and the increasing interest in developing more energy storage device electrodes materials is still a great challenge.

(1) Highly conductive materials should play multi-functional role at this point because they tends to facilitate easy electron transportation during electrochemical processes and also reduces the formation of solid electrolyte interface (SEI) layer. Metal nitrides are promising electrode materials because of their high electrical conductivity. When utilized as single electrodes in LIBs and SCs, they were observed to have high reversibility and capacitance respectively. They also have high coulombic efficiencies indicating that they can reduce the formation of SEI layer in LIBs. However, metal nitrides suffer from poor stability. In order to address this problem, attention were diverted to the synthesis of metal nitride nanostructure materials so as to increase electron transportation and provide short diffusion pathways. [83] In fact, metal nitride nanostructure materials have significantly upgraded the poor stability of metal nitrides. More studies have been demonstrated for ternary metal oxides but few have been reported for metal nitrides in both LIBs and SCs. These ternary nitrides were even proved to be cost effective and also show high capacitance (capacity) and excellent rate capability than the single nitrides. [8, 242]

(2) Hybrid coating and composites also play important role in the development of more conductive and stable electrode materials for LIBs and SCs. [243] Metal nitrides, especially TiN have been successfully coated along with other materials (such as metals, metal oxides and nitrides, conducting polymers etc.) as an inactive conductive materials to stabilized the rapid decreases in the capacity of the materials as in LIBs or as current collectors in SCs. [221, 231] Nevertheless, since TiN have been reported to have high electrical conductivity, low cost, high molar density and superior chemical

resistance, further research are still required to be demonstrated on other transition metal nitrides. The problem of instability of electrode materials has been solved to a certain extent with the coating of carbonanoeous materials. Metal nitrides coated with carbon have been studied not only to improve the stability of the electrode but also increase the capacity (capacitance). [170, 191] It is much promising to utilize such coating method to improve the stability of more metal nitrides. Both carbonaceous materials and metal nitrides were reported to have good electrical conductivities. Their composites might yield excellent stability, attractive rate capability and high capacity. Moreover, more attention should be paid to metal nitride composites and other carbon based materials such as graphene and CNTs. Few works have been reported for such composites. These carbonaceous materials have not only been widely reported as conducting material but also as binder free materials which has significantly improved the stability of other electrode materials. [166, 219] Such improvement still remains vital challenge for metal nitrides.

(3) Furthermore, the development of flexible electronics has attracted great attention due to their thin, lightweight and flexibility. [245] It is high demanded to have flexible devices with high energy density, thus, fabrication of electrode materials with high energy density becomes a vital challenge. Selecting suitable material that can meet up this challenge, metal nitrides were considered as favorable candidates because TiN {Lu, 2012 #6} and VN [190] have been proved to exhibit high energy densities in the fabrication of SSCs and ASCs and also better than many of the reported metal oxides and carbonaceous based materials. However, few researches

have been reported on fabrication of metal nitride SCs with high energy densities and just only one report have been found on LIBs flexible devices based on metal nitride electrodes. [142] Therefore, the development of flexible devices based on metal nitride electrodes is highly desirable and prospective research can also be focused on this field.

Acknowledgements

We acknowledge the financial support from the Natural Science Foundations of China (21273290, and 91323101), the Natural the Research Fund for the Doctoral Program of Higher Education of China (20120171110043), and the Opening Fund of Laboratory Sun Yat-Sen University.

References:

1. J.-M. Tarascon and M. Armand, *Nature*, 2001, **414**, 359.
2. M. Armand and J.-M. Tarascon, *Nature*, 2008, **451**, 652.
3. D. H. Gregory, *The Chemical Record*, 2008, **8**, 229.
4. Z. Song and H. Zhou, *Energy Environ. Sci.*, 2013,**6**, 2280.
5. T. Christen and M. W. Carlen, *J. Power Sources*, 2000, **91**, 210.
6. P. Poizot and F. Dolhem, *Energy Environ. Sci.*, 2011, **4**, 2003.
7. Z. Wang and L. Zhou, *Adv. Mater.*, 2012, **24**, 1903.
8. G. Cui, L. Gu, A. Thomas, L. Fu, P. A. van Aken, M. Antonietti and J. Maier, *ChemPhysChem*, 2010, **11**, 3219.
9. G. Wang, X. Shen, J. Yao and J. Park, *Carbon*, 2009, **47**, 2049.

10. K. T. Lee, J. C. Lytle, N. S. Ergang, S. M. Oh and A. Stein, *Adv. Funct. Mater.*, 2005, **15**, 547.

11. G. Che, B. B. Lakshmi, E. R. Fisher and C. R. Martin, *Nature*, 1998, **393**, 346.

12. B. Guo, X. Wang, P. F. Fulvio, M. Chi, S. M. Mahurin, X. G. Sun and S. Dai, *Adv. Mater.*, 2011, **23**, 4661.

13. S. Li, Y. Luo, W. Lv, W. Yu, S. Wu, P. Hou, Q. Yang, Q. Meng, C. Liu and H. M. Cheng, *Adv. Energy Mater.*, 2011, **1**, 486.

14. J. Chen, L.-n. Xu, W.-y. Li and X.-l. Gou, *Adv. Mater.*, 2005, **17**, 582-586.

15. P.-L. Taberna, S. Mitra, P. Poizot, P. Simon and J.-M. Tarascon, *Nature Mater.*, 2006, **5**, 567-573.

16. L. Li, A. R. O. Raji and J. M. Tour, *Adv. Mater.*, 2013, **25**, 6398.

17. W.-T. Kim, Y. U. Jeong, Y. J. Lee, Y. J. Kim and J. H. Song, *J. Power Sources*, 2013, **244**, 557.

18. S. Dong, X. Chen, X. Zhang and G. Cui, *Coord. Chem. Rev.*, 2013, **257**, 1946-1956.

19. D. Tang, R. Yi, M. L. Gordin, M. Melnyk, F. Dai, S. Chen, J. Song and D. Wang, *J. Mater. Chem. A*, 2014, **2**, 10375.

20. P. Patel, I.-S. Kim and P. Kumta, *Mat. Sci. Eng. B*, 2005, **116**, 347.

21. M. Naguib, J. Halim, J. Lu, K. M. Cook, L. Hultman, Y. Gogotsi and M. W. Barsoum, *J. Am. Chem. Soc.*, 2013, **135**, 15966-.

22. S.-H. Yeon, K.-N. Jung, S. Yoon, K.-H. Shin and C.-S. Jin, *J. Phys. Chem. Solids*, 2013, **74**, 1045.

23. J. T. Lee, Y. Zhao, S. Thieme, H. Kim, M. Oschatz, L. Borchardt, A. Magasinski, W. I. Cho, S. Kaskel and G. Yushin, *Adv. Mater.*, 2013, **25**, 4573.

24. X.-M. Liu, B. Zhang, P.-C. Ma, M. M. Yuen and J.-K. Kim, *Compos. Sci. Tech.*, 2012, **72**, 121.

25. L. Ji, Z. Lin, M. Alcoutlabi and X. Zhang, *Energy Environ. Sci.*, 2011, **4**, 2682.

26. K. H. Seng, M.-h. Park, Z. P. Guo, H. K. Liu and J. Cho, *Nano Lett.*, 2013, **13**, 1230.

27. M. Zhi, C. Xiang, J. Li, M. Li and N. Wu, *Nanoscale*, 2013, **5**, 72.

28. E. Antolini, *Solid State Ionics*, 2004, **170**, 159.

29. S. Luo, K. Wang, J. Wang, K. Jiang, Q. Li and S. Fan, *Adv. Mater.*, 2012, **24**, 2294.

30. A. R. Armstrong and P. G. Bruce, *Nature*, 1996, **381**, 499.

31. S. Chen, F. Cao, F. Liu, Q. Xiang, X. Feng, L. Liu and G. Qiu, *RSC Adv.*, 2014, **4**, 13693.

32. D.-H. Baek, J.-K. Kim, Y.-J. Shin, G. S. Chauhan, J.-H. Ahn and K.-W. Kim, *J. Power Sources*, 2009, **189**, 59.

33. G. Kobayashi, A. Yamada, S.-i. Nishimura, R. Kanno, Y. Kobayashi, S. Seki, Y. Ohno and H. Miyashiro, *J. Power Sources*, 2009, **189**, 397.

34. A. D. Pasquier, H. E. Unalan, A. Kanwal, S. Miller and M. Chhowalla, *Appl. Phys. Lett.*, 2005, **87**, 203511.

35. Y.-K. Kim and D.-H. Min, *Langmuir*, 2009, **25**, 11302.

36. T. Zhai, F. Wang, M. H. Yu, S. Xie, C. Liang, C. Li, F. Xiao, R. Tang, Q. Wu and X. H. Lu, *Nanoscale*, 2013, **5**, 6790.

37. D. S. Hecht, L. Hu and G. Irvin, *Advanced Materials*, 2011, **23**, 1482.

38. K. S. Ryu, K. M. Kim, N.-G. Park, Y. J. Park and S. H. Chang, *J. Power Sources*, 2002, **103**, 305.

39. M. Yu, Y. Zeng, C. Zhang, X. Lu, C. Zeng, C. Yao, Y. Yang and Y. Tong, *Nanoscale*, 2013, **5**, 10806.

40. M. S. Whittingham, *Prog. Solid State Chem.*, 1978, **12**, 41.

41. B. Di Pietro, M. Patriarca and B. Scrosati, *Synthetic Met.*, 1982, **5**, 1-9.

42. M. Yu, T. Zhai, X. Lu, X. Chen, S. Xie, W. Li, C. Liang, W. Zhao, L. Zhang and Y. Tong, *J. Power Sources*, 2013, **239**, 64.

43. L. Yuan, X.-H. Lu, X. Xiao, T. Zhai, J. Dai, F. Zhang, B. Hu, X. Wang, L. Gong and J. Chen, *ACS Nano*, 2011, **6**, 656.

44. Z. Tang, C. h. Tang and H. Gong, *Adv. Funct. Mater.*, 2012, **22**, 1272.

45. J. Liu, J. Jiang, C. Cheng, H. Li, J. Zhang, H. Gong and H. J. Fan, *Adv. Mater.*, 2011, **23**, 2076.

46. S.-F. Zheng, J.-S. Hu, L.-S. Zhong, W.-G. Song, L.-J. Wan and Y.-G. Guo, *Chem. Mater.*, 2008, **20**, 3617.

47. X. Lu, T. Zhai, X. Zhang, Y. Shen, L. Yuan, B. Hu, L. Gong, J. Chen, Y. Gao and J. Zhou, *Adv. Mater.*, 2012, **24**, 938.

48. P. Poizot, S. Laruelle, S. Grugeon, L. Dupont and J. Tarascon, *Nature*, 2000, **407**, 496.

49. V. Etacheri, R. Marom, R. Elazari, G. Salitra and D. Aurbach, *Energy Environ. Sci.*, 2011, **4**, 3243.
50. D. Deng, M. G. Kim, J. Y. Lee and J. Cho, *Energy Environ. Sci.*, 2009, **2**, 818.
51. W. Wei, X. Cui, W. Chen and D. G. Ivey, *Chem. Soc. Rev.*, 2011, **40**, 1697.
52. X. Huang, X. Qi, F. Boey and H. Zhang, *Chem. Soc. Rev.*, 2012, **41**, 666.
53. Y. Huang, J. Liang and Y. Chen, *Small*, 2012, **8**, 1805.
54. S. Elder, L. H. Doerrer, F. DiSalvo, J. Parise, D. Guyomard and J. Tarascon, *Chem. Mater.*, 1992, **4**, 928-937.
55. S. Dong, X. Chen, L. Gu, X. Zhou, H. Wang, Z. Liu, P. Han, J. Yao, L. Wang, G. Cui and L. Chen, *Mater. Res. Bull.*, 2011, **46**, 835-839.
56. Q. Sun and Z.-W. Fu, *Electrochim. Acta*, 2008, **54**, 403-409.
57. D. K. Nandi, U. K. Sen, D. Choudhury, S. Mitra and S. K. Sarkar, *ACS Appl. Mater. Inter.*, 2014, **6**, 6606–6615.
58. Q. Sun and Z.-W. Fu, *Electrochem. Solid-State Lett.*, 2008, **11**, A233-A237.
59. F. Gillot, J. Oró-Solé and M. R. Palacín, *J. Mater. Chem.*, 2011, **21**, 9997-10002.
60. D. Choi and P. N. Kumta, *J. Am. Ceram. Soc.*, 2011, **94**, 2371-2378.
61. D. Choi and P. N. Kumta, *J. Am. Ceram. Soc.*, 2007, **90**, 3113-3120.
62. A. Hector and W. Levason, *Coordin. Chem. Rev.*, 2013, **257**, 1945.
63. D. J. Ham and J. S. Lee, *Energies*, 2009, **2**, 873-899.
64. S. Ramanathan and S. Oyama, *J. Phys. Chem.*, 1995, **99**, 16365-16372.

65. A. Zerr, G. Miehe, G. Serghiou, M. Schwarz, E. Kroke, R. Riedel, H. Fueß, P. Kroll and R. Boehler, *Nature*, 1999, **400**, 340-342.

66. K. Leinenweber, M. O'keeffe, M. Somayazulu, H. Hubert, P. McMillan and G. Wolf, *Chem. Euro. J.*, 1999, **5**, 3076-3078.

67. G. Serghiou, G. Miehe, O. Tschauner, A. Zerr and R. Boehler, *J. Chem. Phys.*, 1999, **111**, 4659.

68. B. Mazumder and A. L. Hector, *J. Mater. Chem.*, 2009, **19**, 4673-4686.

69. X. Lu, T. Liu, T. Zhai, G. Wang, M. Yu, S. Xie, Y. Ling, C. Liang, Y. Tong and Y. Li, *Adv. Energy Mater.*, 2014, **4**, 1300994.

70. X. Lu, G. Wang, T. Zhai, M. Yu, S. Xie, Y. Ling, C. Liang, Y. Tong and Y. Li, *Nano Lett.*, 2012, **12**, 5376-5381.

71. X. Lu, M.-H. Yu, T. Zhai, G. Wang, S. Xie, T. Lu, C. Liang, Y.-X. Tong and Y. Li, *Nano Lett.*, 2013, **13**, 2626-2633.

72. Z.-W. Fu, Y. Wang, X.-L. Yue, S.-L. Zhao and Q.-Z. Qin, *J. Phys. Chem. B*, 2004, **108**, 2236-2244.

73. Q. Sun and Z.-W. Fu, *Appl. Surf. Sci.*, 2012, **258**, 3197-3201.

74. M. D. Aguas, A. M. Nartowski, I. P. Parkin, M. MacKenzie and A. J. Craven, *J. Mater. Chem.*, 1998, **8**, 1875-1880.

75. E. G. Gillan and R. B. Kaner, *J. Mater. Chem.*, 2001, **11**, 1951-1956.

76. E. G. Gillan and R. B. Kaner, *Chem. Mater.*, 1996, **8**, 333-343.

77. E. G. Gillan and R. B. Kaner, *Inorg. Chem.*, 1994, **33**, 5693-5700.

78. F. Xu, Y. Xie, X. Zhang, S. Zhang and L. Shi, *New J. Chem.*, 2003, **27**, 565-567.

79. F. Cheng, S. M. Kelly, S. Clark, N. A. Young, S. J. Archibald, J. S. Bradley and F. Lefebvre, *Chem. Mater.*, 2005, **17**, 5594-5602.

80. G. Chaplais and S. Kaskel, *J. Mater. Chem.*, 2004, **14**, 1017-1025.

81. A. W. Jackson and A. L. Hector, *J. Mater. Chem.*, 2007, **17**, 1016-1022.

82. P. Kroll, T. Schröter and M. Peters, *Angew. Chem. Int. Edit.*, 2005, **44**, 4249-4254.

83. P. Kroll, *Phys. Rev. Lett.*, 2003, **90**, 125501.

84. P. Kroll, *Journal of Physics: Condensed Matter*, 2004, **16**, S1235.

85. N. Suzuk, R. B. Cervera, T. Ohnishi and K. Takada, *J. Power Sources*, 2013, **231**, 186-189.

86. B. Das, M. Reddy, P. Malar, T. Osipowicz, G. Subba Rao and B. Chowdari, *Solid State Ionics*, 2009, **180**, 1061-1068.

87. Z. Stoeva, R. Gomez, A. G. Gordon, M. Allan, D. H. Gregory, G. B. Hix and J. J. Titman, *J. Am. Chem. Soc.*, 2004, **126**, 4066-4067.

88. A. S. Powell, Z. Stoeva, R. I. Smith, D. H. Gregory and J. J. Titman, *Phys. Chem. Chem. Phys.*, 2011, **13**, 10641-10647.

89. J. L. Rowsell, V. Pralong and L. F. Nazar, *J. Am. Chem. Soc.*, 2001, **123**, 8598-8599.

90. D. H. Gregory, P. M. O'Meara, A. G. Gordon, D. J. Siddons, A. J. Blake, M. G. Barker, T. A. Hamor and P. P. Edwards, *J. Alloy. Compd.*, 2001, **317**, 237-244.

91. Z. Stoeva, R. Gomez, D. H. Gregory, G. B. Hix and J. J. Titman, *Dalton T.*, 2004, 3093-3097.

92. Y. Takeda, M. Nishijima, M. Yamahata, K. Takeda, N. Imanishi and O. Yamamoto, *Solid State Ionics*, 2000, **130**, 61-69.

93. T. Shodai, Y. Sakurai and T. Suzuki, *Solid State Ionics*, 1999, **122**, 85-93.

94. M. Nishijima, Y. Takeda, N. Imanishi, O. Yamamoto and M. Takano, *J. Solid State Chem.*, 1994, **113**, 205-210.

95. A. Rabenau and H. Schulz, *J. Less Common Met.*, 1976, **50**, 155-159.

96. Y. Liu, T. Matsumura, N. Imanishi, T. Ichikawa, A. Hirano and Y. Takeda, *Electrochem. Commun.s*, 2004, **6**, 632-636.

97. T. Shodai, S. Okada, S.-i. Tobishima and J.-i. Yamaki, *Solid State Ionics*, 1996, **86**, 785-789.

98. T. Shodai, S. Okada, S. Tobishima and J. Yamaki, *Journal of power sources*, 1997, **68**, 515-518.

99. M. Nishijima, T. Kagohashi, M. Imanishi, Y. Takeda, O. Yamamoto and S. Kondo, *Solid State Ionics*, 1996, **83**, 107-111.

100. M. Nishijima, T. Kagohashi, Y. Takeda, M. Imanishi and O. Yamamoto, *J. Power sources*, 1997, **68**, 510-514.

101. E. Panabière, N. Emery, S. Bach, J. Pereira-Ramos and P. Willmann, *Corros. Sci.*, 2012, **58**, 237-241.

102. M. Nishijima, N. Tadokoro, Y. Takeda, N. Imanishi and O. Yamamoto, *J. Electrochem. Soc.*, 1994, **141**, 2966-2971.

103. J. Cabana, C. M. Ionica-Bousquet, C. P. Grey and M. R. Palacín, *Electrochem. Commun.*, 2010, **12**, 315-318.

104. Z. Wen, K. Wang, L. Chen and J. Xie, *Electrochem. Commun.*, 2006, **8**, 1349-1352.

105. E. Panabiere, N. Emery, S. Bach, J.-P. Pereira-Ramos and P. Willmann, *Electrochim. Acta*, 2013, **97**, 393-397.

106. Y.-M. Kang, S.-C. Park, Y.-S. Kang, P. S. Lee and J.-Y. Lee, *Solid State Ionics*, 2003, **156**, 263-273.

107. P. W. Gruber, P. A. Medina, G. A. Keoleian, S. E. Kesler, M. P. Everson and T. J. Wallington, *J. Ind. Eco.*, 2011, **15**, 760-775.

108. N. Pereira, L. Dupont, J. Tarascon, L. Klein and G. Amatucci, *J. Electrochem. Soc.*, 2003, **150**, A1273-A1280.

109. N. Pereira, L. Klein and G. Amatucci, *J. Electrochem. Soc.*, 2002, **149**, A262-A271.

110. M. Wu, Z. Wen, Y. Liu, X. Wang and L. Huang, *J. Power Sources*, 2011, **196**, 8091-8097.

111. N. Futamura, T. Ichikawa, N. Imanishi, Y. Takeda and O. Yamamoto, in *Meeting Abstracts*, The Electrochemical Society, 2012, pp. 1137-1137.

112. C. Desjardins, *J. Power Sources*, 1988, **12**, 489.

113. D. Aurbach, E. Zinigrad, H. Teller, Y. Cohen, G. Salitra, H. Yamin, P. Dan and E. Elster, *J. Electrochem. Soc.*, 2002, **149**, A1267-A1277.

114. R. Singh and V. Singh, *Phys. Chem. Liq.*, 1991, **22**, 235-243.

115. J. C. Schön, M. A. Wevers and M. Jansen, *J. Mater. Chem.*, 2001, **11**, 69-77.

116. J. Zhang, M.-A. Pilette, F. Cuevas, T. Charpentier, F. Mauri and M. Latroche, *J. Phys. Chem. C*, 2009, **113**, 21242-21252.

117. B. Neudecker, R. Zuhr and J. Bates, *J. Power Sources*, 1999, **81**, 27-32.

118. Y. Wang, Z.-W. Fu, X.-L. Yue and Q.-Z. Qin, *J. Electrochem. Soc.*, 2004, **151**, E162-E167.

119. J. Bates, N. Dudney, B. Neudecker, A. Ueda and C. Evans, *Solid State Ionics*, 2000, **135**, 33-45.

120. K. Park, Y. Park, M. Kim, J. Son, H. Kim and S. Kim, *J. Power Sources*, 2001, **103**, 67-71.

121. B. Neudecker, R. Zuhr and J. Bates, *Battery Materials*, 2000, **99**, 295-304.

122. N. Pereira, M. Balasubramanian, L. Dupont, J. McBreen, L. Klein and G. Amatucci, *J. Electrochem. Soc.*, 2003, **150**, A1118-A1128.

123. Q. Sun and Z.-W. Fu, *Electrochem. solid-state Lett.*, 2007, **10**, A189-A193.

124. Y. Zhang, Z.-W. Fu and Q.-Z. Qin, *Electrochem. Commun.*, 2004, **6**, 484-491.

125. L. Toth, *and references therein*, 1992, 87.

126. E. Gregoryanz, C. Sanloup, M. Somayazulu, J. Badro, G. Fiquet, H.-K. Mao and R. J. Hemley, *Nature Mater.*, 2004, **3**, 294-297.

127. J. C. Crowhurst, A. F. Goncharov, B. Sadigh, C. L. Evans, P. G. Morrall, J. L. Ferreira and A. Nelson, *Science*, 2006, **311**, 1275-1278.

128. S. Bouhtiyya, R. Lucio Porto, B. Laïk, P. Boulet, F. Capon, J. Pereira-Ramos, T. Brousse and J. Pierson, *Scripta Materialia*, 2013, **9**, 659-662.

129. A. L. Ivanovskii, *Russ. Chem. Rev.*, 2009, **78**, 303-318.

130. Q. Sun, W.-J. Li and Z.-W. Fu, *Solid State Sci.*, 2010, **12**, 397-403.

131. W. Li, C.-Y. Cao, C.-Q. Chen, Y. Zhao, W.-G. Song and L. Jiang, *Chem. Commun.*, 2011, **47**, 3619-3621.

132. P. G. Bruce, B. Scrosati and J. M. Tarascon, *Angew. Chem. Int. Edit.*, 2008, **47**, 2930-2946.

133. C. Jiang, E. Hosono and H. Zhou, *Nano Today*, 2006, **1**, 28-33.

134. K. T. Lee and J. Cho, *Nano Today*, 2011, **6**, 28-41.

135. Y. G. Guo, J. S. Hu and L. J. Wan, *Adv. Mater.*, 2008, **20**, 2878-2887.

136. Y. Wang, H. Li, P. He, E. Hosono and H. Zhou, *Nanoscale*, 2010, **2**, 1294-1305.

137. H. B. Wu, J. S. Chen, H. H. Hng and X. W. D. Lou, *Nanoscale*, 2012, **4**, 2526-2542.

138. S. W. Lee, B. M. Gallant, H. R. Byon, P. T. Hammond and Y. Shao-Horn, *Energy Environ. Sci.*, 2011, **4**, 1972-1985.

139. C. X. Guo, M. Wang, T. Chen, X. W. Lou and C. M. Li, *Adv. Energy Mater.*, 2011, **1**, 736-741.

140. L.-F. Cui, L. Hu, J. W. Choi and Y. Cui, *ACS Nano*, 2010, **4**, 3671-3678.

141. M. V. Reddy, G. Prithvi, K. P. Loh and B. V. R. Chowdari, *ACS Appl. Mater. Inter.*, 2014, **6**, 680-690

142. B. Das, M. Reddy, G. S. Rao and B. Chowdari, *J. Mater. Chem.*, 2012, **22**, 17505-17510.

143. Y. Takeda and J. Yang, *J. Power Sources*, 2001, **97**, 244-246.

144. B. Das, M. Reddy, G. S. Rao and B. Chowdari, *RSC Adv.*, 2012, **2**, 9022-9028.

145. M.-S. Balogun, M. Yu, C. Li, T. Zhai, Y. Liu, X. Lu and Y. Tong, *J. Mater. Chem. A*, 2014, **2**, 10825-10829.

146. S. Dong, H. Wang, L. Gu, X. Zhou, Z. Liu, P. Han, Y. Wang, X. Chen, G. Cui and L. Chen, *ChemPhyChem*, 2011, **11**, 3219-3223.

147. P. N. Kumta and G. Blomgren, *Mater. Electrochem. Energy Con. Sto.*, 2002, 249-258.

148. I. s. Kim, P. Kumta and G. Blomgren, *Electrochem. Solid-State Lett.*, 2000, **3**, 493-496.

149. J. H. Bang and K. S. Suslick, *Adv. Mater.*, 2009, **21**, 3186-3190.

150. C. J. Carmalt, A. H. Cowley, R. D. Culp, R. A. Jones, Y.-M. Sun, B. Fitts, S. Whaley and H. W. Roesky, *Inorg. Chem.*, 1997, **36**, 3108-3112.

151. S. Kaskel, K. Schlichte, G. Chaplais and M. Khanna, *J. Mater. Chem.*, 2003, **13**, 1496-1499.

152. M.-A. Nicolet, *Thin Solid Films*, 1978, **52**, 415-443.

153. J. Liu, S. Tang, Y. Lu, G. Cai and X. Chen, *Energy Environ. Sci.*, 2013,**6**, 2691-2697.

154. E. M. Sorensen, S. J. Barry, H.-K. Jung, J. M. Rondinelli, J. T. Vaughey and K. R. Poeppelmeier, *Chem. Mater.*, 2006, **18**, 482-489.

155. C. Jiang, Y. Zhou, I. Honma, T. Kudo and H. Zhou, *J. Power Sources*, 2007, **166**, 514-518.

156. S. C. Lee, S. M. Lee, J. W. Lee, J. B. Lee, S. M. Lee, S. S. Han, H. C. Lee and H. J. Kim, *J. Phys. Chem. C*, 2009, **113**, 18420-18423.

157. L. Cheng, J. Yan, G.-N. Zhu, J.-Y. Luo, C.-X. Wang and Y.-Y. Xia, *J. Mater. Chem.*, 2010, **20**, 595-602.

158. S. Huang, Z. Wen, B. Lin, J. Han and X. Xu, *J. Alloy. Compd.*, 2008, **457**, 400-403.

159. M. Q. Snyder, S. A. Trebukhova, B. Ravdel, M. C. Wheeler, J. DiCarlo, C. P. Tripp and W. J. DeSisto, *J. Power Sources*, 2007, **165**, 379-385.

160. K.-S. Park, A. Benayad, D.-J. Kang and S.-G. Doo, *J. Am. Chem. Soc.*, 2008, **130**, 14930-14931.

161. J. Zhang, J. Zhang, W. Cai, F. Zhang, L. Yu, Z. Wu and Z. Zhang, *J. Power Sources*, 2012, **211**, 133-139.

162. H. Han, T. Song, J.-Y. Bae, L. F. Nazar, H. Kim and U. Paik, *Energy Environ. Sci.*, 2011, **4**, 4532-4536.

163. Y. Li, Y. Yan, H. Ming and J. Zheng, *Appl. Surf. Sci.*, 2014, **305**, 683-688.

164. D.-H. Ha, M. A. Islam and R. D. Robinson, *Nano Lett.*, 2012, **12**, 5122-5130.

165. G. Q. Zhang, H. B. Wu, H. E. Hoster, M. B. Chan-Park and X. W. D. Lou, *Energy Environ.l Sci.*, 2012, **5**, 9453-9456.

166. C. Ban, Z. Wu, D. T. Gillaspie, L. Chen, Y. Yan, J. L. Blackburn and A. C. Dillon, *Adv. Mater.*, 2010, **22**, E145-E149.

167. H. Wu, S. A. Shevlin, Q. Meng, W. Guo, Y. Meng, K. Lu, Z. Wei and Z. Guo, *Adv. Mater.*, 2014, **26**, 3338-3343.

168. A. K. Geim and K. S. Novoselov, *Nature Mater.*, 2007, **6**, 183-191.

169. S. Stankovich, D. A. Dikin, G. H. Dommett, K. M. Kohlhaas, E. J. Zimney, E. A. Stach, R. D. Piner, S. T. Nguyen and R. S. Ruoff, *Nature*, 2006, **442**, 282-286.

170. E. Hwang, S. Adam and S. D. Sarma, *Phys. Rev. Lett.*, 2007, **98**, 186806.

171. M. Liang and L. Zhi, *J. Mater. Chem.*, 2009, **19**, 5871-5878.

172. Z.-S. Wu, W. Ren, L. Xu, F. Li and H.-M. Cheng, *ACS Nano*, 2011, **5**, 5463-5471.

173. D. Lei, T. Yang, B. Qu, J. Ma, Q. Li, L. Chen and T. Wang, *Sci. Ed.*, 2014, **2**, 1-4.

174. K. Zhang, H. Wang, X. He, Z. Liu, L. Wang, L. Gu, H. Xu, P. Han, S. Dong and C. Zhang, *J. Mater. Chem.*, 2011, **21**, 11916-11922.

175. Y. Yue, P. Han, X. He, K. Zhang, Z. Liu, C. Zhang, S. Dong, L. Gu and G. Cui, . *Mater. Chem.*, 2012, **22**, 4938-4943.

176. X. Lu, M. Yu, G. Wang, Y. Tong and Y. Li, *Energy Environ. Sci.*, 2014, **7**, 2160-2181.

177. L. Li, Z. Wu, S. Yuan and X. ZHANG, *Energy Environ. Sci.*, 2014, **7**, 2101-2122.

178. G. Zhou, F. Li and H.-M. Cheng, *Energy Environ. Sci.*, 2014,**7**, 1307-1338.

179. S.-Y. Lee, K.-H. Choi, W.-S. Choi, Y. H. Kwon, H.-R. Jung, H.-C. Shin and J. Y. Kim, *Energy Environ. Sci.*, 2013, **6**, 2414-2423.

180. L. Hu, H. Wu, F. La Mantia, Y. Yang and Y. Cui, *ACS Nano*, 2010, **4**, 5843-5848.

181. L. Jabbour, M. Destro, C. Gerbaldi, D. Chaussy, N. Penazzi and D. Beneventi, *J. Mater. Chem.*, 2012, **22**, 3227-3233.

182. N. Li, Z. Chen, W. Ren, F. Li and H.-M. Cheng, *P. Natl. Acad. Sci. USA*, 2012, **109**, 17360-17365.

183. L. Noerochim, J.-Z. Wang, S.-L. Chou, D. Wexler and H.-K. Liu, *Carbon*, 2012, **50**, 1289-1297.

184. W. Li, X. Wang, B. Liu, S. Luo, Z. Liu, X. Hou, Q. Xiang, D. Chen and G. Shen, *Chem. Euro. J.*, 2013, **19**, 8650-8656.

185. H. Yu, C. Zhu, K. Zhang, Y.-J. Chen, C. Li, P. Gao and Q. Ouyang, *J. Mater. Chem. A*, 2014, **2**, 4551-4557.

186. E. Bailey, N. M. T. Ray, A. L. Hector, P. Crozier, W. T. Petuskey and P. F. McMillan, *Materials*, 2011, **4**, 1747-1762.

187. L. Xu, S. Li, Y. Zhang and Y. Zhai, *Nanoscale*, 2012, **4**, 4900-4915.

188. J. Yang, Y. Takeda, N. Imanishi and O. Yamamoto, *Electrochim. Acta*, 2001, **46**, 2659-2664.

189. P. Simon and Y. Gogotsi, *Na.t Mater.*, 2008, **7**, 845-854.

190. H. Jiang, J. Ma and C. Li, *Adv. Mater.*, 2012, **24**, 4197-4202.

191. M. Epifani, T. Chávez-Capilla, T. Andreu, J. Arbiol, J. Palma, J. R. Morante and R. Díaz, *Energy Environ. Sci.*, 2012, **5**, 7555-7558.

192. T. Y. Kosolapova, *Production, Applications (Hemisphere, New York, 1990)*, 1990.

193. X. Zhou, H. Chen, D. Shu, C. He and J. Nan, *J. Phy. Chem. Solids*, 2009, **70**, 495-500.

194. D. Choi and P. N. Kumta, *Electrochem. Solid-State Lett.*, 2005, **8**, A418-A422.

195. P. Jampani, A. Manivannan and P. N. Kumta, *J. Electrochem. Soc. Inter.*, 2010, **19**, 57-62.

196. M. Wixom, D. Tarnowski, J. Parker, J. Lee, P. Chen, I. Song and L. Thompson, in *Materials Research Society Symposium Proceedings*, Cambridge Univ Press, 1998, pp. 643-654.

197. S. Bouhtiyya, R. Lucio-Porto, J.-B. Ducros, P. Boulet, F. Capon, T. Brousse and J.-F. Pierson, in *Meeting Abstracts*, The Electrochemical Society, 2012, pp. 494-494.

198. T. C. Liu, W. Pell, B. Conway and S. Roberson, *J. Electrochem. Soc.*, 1998, **145**, 1882-1888.

199. X.-l. LI, Y. XING, H. WANG, H.-l. WANG, W.-d. WANG and X.-y. CHEN, *Trans. Nonferrous Met. Soc. China*, 2009, **19**, 620-625.

200. Y.-J. B. Ting, K. Lian and N. Kherani, *ECS Trans.*, 2011, **35**, 133-139.

201. C. Chen, D. Zhao and X. Wang, *Mater. Chem. Phys.*, 2006, **97**, 156-161.

202. Y. X. L. Xueliang, *Anhui Chem. Ind.*, 2002, **2**, 012.

203. L. Xue_liang, L. Dao_rong, W. Hua_lin, H. Jian_bo and Z. Yun_guei, *Electrochemistry*, 2002, **3**, 015.

204. X.-l. LI, D.-l. ZHAO, Y.-h. YOU and D.-r. LU, *Nonferrous Met.*, 2004, **4**, 007.

205. Z. D. L. Xueliang, *Anhui Chem. Ind.*, 2004, **4**, 013.

206. C. Chen, D. Zhao, D. Xu and X. Wang, *Mater. Chem. Phys.*, 2006, **95**, 84-88.

207. S. Dong, X. Chen, L. Gu, L. Zhang, X. Zhou, Z. Liu, P. Han, H. Xu, J. Yao and X. Zhang, *Biosens. Bioelectron.*, 2011, **26**, 4088-4094.

208. I. Milošv, H. H. Strehblow, B. Navinšek and M. Metikoš‐Hukovió, *Surf. Inter. Anal.*, 1995, **23**, 529-539.

209. B. Avasarala and P. Haldar, *Electrochim. Acta*, 2010, **55**, 9024-9034.

210. D. Sun, J. Lang, X. Yan, L. Hu and Q. Xue, *J. Solid State Chem.*, 2011, **184**, 1333-1338.

211. S. Dong, X. Chen, L. Gu, X. Zhou, H. Xu, H. Wang, Z. Liu, P. Han, J. Yao and L. Wang, *ACS Appl. Mater. Inter.*, 2010, **3**, 93-98.

212. D. Choi and P. N. Kumta, *J. Electrochem. Soc.*, 2006, **153**, A2298-A2303.

213. Y. Xie and X. Fang, *Electrochim. Acta*, 2014, **120**, 273-283.

214. H. Li and H. Zhou, *Chem. Commun.*, 2012, **48**, 1201-1217.

215. K. Jost, C. R. Perez, J. K. McDonough, V. Presser, M. Heon, G. Dion and Y. Gogotsi, *Energy Environ. Sci.*, 2011, **4**, 5060-5067.

216. M. Inagaki, *Carbon*, 2012, **50**, 3247-3266.

217. E. Ramasamy, C. Jo, A. Anthonysamy, I. Jeong, J. K. Kim and J. Lee, *Chem. Mater.*, 2012, **24**, 1575-1582.

218. D. Choi, G. E. Blomgren and P. N. Kumta, *Adv. Mater.*, 2006, **18**, 1178-1182.

219. A. M. Glushenkov, D. Hulicova-Jurcakova, D. Llewellyn, G. Q. Lu and Y. Chen, *Chem. Mater.*, 2009, **22**, 914-921.

220. C. Peng, S. Zhang, D. Jewell and G. Z. Chen, *Prog. Nat. Sci.*, 2008, **18**, 777-788.

221. L. L. Zhang and X. Zhao, *Chem. Soc. Rev.*, 2009, **38**, 2520-2531.

222. S. Dong, X. Chen, L. Gu, X. Zhou, L. Li, Z. Liu, P. Han, H. Xu, J. Yao and H. Wang, *Energy Environ. Sci.*, 2011, **4**, 3502-3508.

223. K. Huang and M. Wan, *Chem. Mater.*, 2002, **14**, 3486-3492.

224. B. A. Deore, I. Yu and M. S. Freund, *J. Am. Chem. Soc.*, 2004, **126**, 52-53.

225. Y. Qiu and L. Gao, *J. Phy. Chem. B*, 2005, **109**, 19732-19740.

226. C. Xia, Y. Xie, Y. Wang, W. Wang, H. Du and F. Tian, *J. Appl. Electrochem.*, 2013, **43**, 1225-1233.

227. H. Du, Y. Xie, C. Xia, W. Wang and F. Tian, *New J. Chem.*, 2014, **38**, 1284-1293.

228. X. Peng, K. Huo, J. Fu, X. Zhang, B. Gao and P. K. Chu, *Chem. Commun.*, 2013, **49**, 10172-10174.

229. E. Frackowiak and F. Beguin, *Carbon*, 2002, **40**, 1775-1787.

230. L. Jiang and L. Gao, *J. Mater. Chem.*, 2005, **15**, 260-266.

231. L. Jiang and L. Gao, *J. Am. Ceram. Soc.*, 2006, **89**, 156-161.

232. S. A. Sherrill, J. Duay, Z. Gui, P. Banerjee, G. W. Rubloff and S. B. Lee, *Phys. Chem. Chem. Phys.*, 2011, **13**, 15221-15226.

233. C. Shang, S. Dong, S. Wang, D. Xiao, P. Han, X. Wang, L. Gu and G. Cui, *ACS Nano*, 2013, **7**, 5430-5436.

234. T.-T. Chen, H.-P. Liu, Y.-J. Wei, I.-C. Chang, M.-H. Yang, Y.-S. Lin, K.-L. Chan, H.-T. Chiu and C.-Y. Lee, *Nanoscale*, 2014, **6**, 5106-5109.

235. G. D. Moon, J. B. Joo, M. Dahl, H. Jung and Y. Yin, *Adv. Funct. Mater.*, 2014, **24**, 848-856.

236. X. Zhou, C. Shang, L. Gu, S. Dong, X. Chen, P. Han, L. Li, J. Yao, Z. Liu and H. Xu, *ACS Appl. Mater. Inter.*, 2011, **3**, 3058-3063.

237. D. Shu, C. Lv, F. Cheng, C. He, K. Yang, J. Nan and L. Long, *Int. J. Electrochem. Sci*, 2013, **8**, 1209-1225.

238. F. Cheng, C. He, D. Shu, H. Chen, J. Zhang, S. Tang and D. E. Finlow, *Mater. Chem. Phys.*, 2011, **131**, 268-273.

239. C. M. Ghimbeu, E. Raymundo-Piñero, P. Fioux, F. Béguin and C. Vix-Guterl, *J. Mater. Chem.*, 2011, **21**, 13268-13275.

240. L. Zhang, C. M. Holt, E. J. Luber, B. C. Olsen, H. Wang, M. Danaie, X. Cui, X. Tan, V. W. Lui and W. P. Kalisvaart, *J. Phys. Chem. C*, 2011, **115**, 24381-24393.

241. Z.-H. Gao, H. Zhang, G.-P. Cao, M.-F. Han and Y.-S. Yang, *Electrochim. Acta*, 2013, **87**, 375-380.

242. X. Xiao, X. Peng, H. Jin, T. Li, C. Zhang, B. Gao, B. Hu, K. Huo and J. Zhou, *Adv. Mater.*, 2013, **25**, 5091-5097.

243. H. Pang, S. J. Ee, Y. Dong, X. Dong and P. Chen, *ChemElectroChem*, 2014.

244. H. Yi, X. Chen, H. Wang and X. Wang, *Electrochim. Acta*, 2014, **116**, 372-378

245. M.-S. Balogun, C. Li, Y. Zeng, M. Yu, Q. Wu, M. Wu, X. Lu and Y. Tong, *J. Power Sources*, 2014, **272**, 946-953.

Recent Advances in Metal Nitrides as High-Performance Electrode Materials for Energy Storage Devices

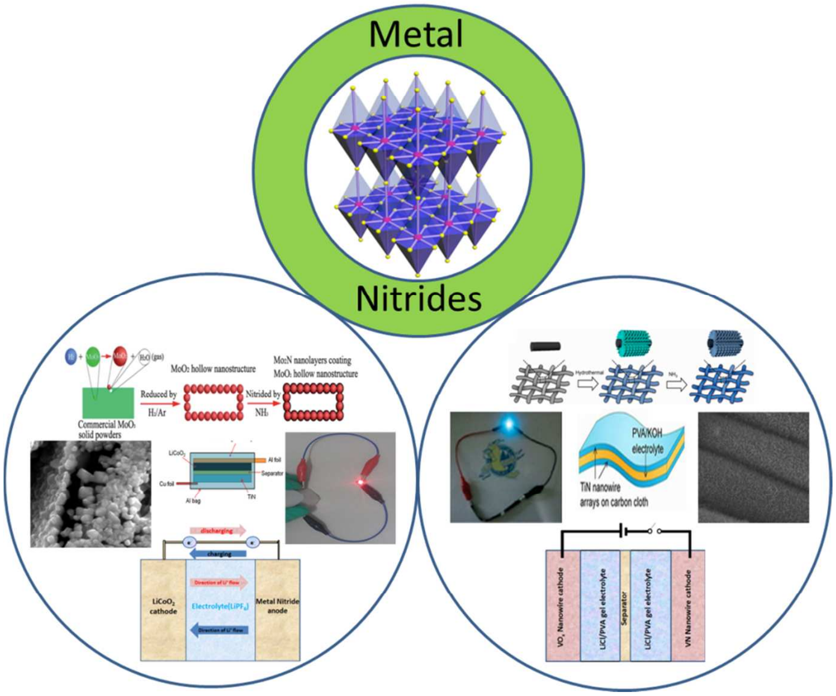

This review highlights the progress and development of metal nitrides as electrode material for energystorage devices